UNIVERSITY OF THE
WITWATERSRAND,
JOHANNESBURG

Monocyte-to-Macrophage Differentiation with 1,25-Dihydroxyvitamin D_3 Potentially Enhances Macrophage Polarisation and Function in THP-1 Cells

by

Janet Julius Wasinda

(2781145)

Dissertation

Submitted in fulfilment of the requirements for the degree of

Master of Science

in

Molecular and Cell Biology

in the Faculty of Science, University of the Witwatersrand, Johannesburg, South Africa

Supervisor: Dr Vanessa Meyer

Co-Supervisor: Dr Nikki L. Gentle

May 2025

DECLARATION

I, **Janet Julius Wasinda** (**2781145**), am a student registered for the degree of **Master of Science**.

I hereby declare the following:

• I am aware that plagiarism (the use of someone else's work without their permission and/or without acknowledging the original source) is wrong.

• I confirm that the work submitted for assessment for the above degree is my own unaided work except where explicitly indicated otherwise and acknowledged. In this context, I understand that the use of editing services is considered aided work and must be declared.

• I have not submitted this work before for any other degree or examination at this or any other University.

• The information used in the Dissertation **HAS NOT** been obtained by me while employed by, or working under the aegis of, any person or organisation other than the University.

• I have followed the required conventions in referencing the thoughts and ideas of others.

• I understand that the University of the Witwatersrand may take disciplinary action against me if there is a belief that this is not my own unaided work or that I have failed to acknowledge the source of the ideas or words in my writing.

Janet Julius Wasinda (2781145)

Date: **28 May 2025**

To God Almighty for the gift of life and hope.

To my Dad, for being my greatest cheerleader. You painfully left before I could complete my work and see you. Even in death, I hear your voice encouraging and praying for me. Thank you for your unconditional love. I love you deeply and miss you greatly.

ACKNOWLEDGEMENTS

To Dr. Meyer, words are not enough to say thank you for giving me a chance, and for making my growth journey bearable and worth it. I am particularly grateful for your kindness, encouragement, patience and care. I am privileged to have you as my supervisor.

To Dr. Gentle, thank you very much for your honest feedback and encouragement throughout my work. I am grateful for your support.

My deepest gratitude to Bronwyn, I am grateful for your kind support, for training me on the lab techniques, answering my many questions and for trusting me to contribute to your publication. To Kiara and Caitlyn, I am very grateful for your kindness and support always, and for sharing your knowledge with me, you made settling into the lab and the whole program much easier. To Nikita and Dana, I am grateful for your support and encouragement always. You made the lab a safe space. To the entire immunomics lab, thank you for an exciting learning opportunity, especially but not limited to our journal club engagements.

To the Mandela Rhodes Foundation, my profound gratitude for funding my entire master's program and the leadership training. I made it here and this far because you believed in me.

To my loving family, Mum, Precious, Stephen, Favour and Joseph, you have been my rock, thank you for your prayers, encouragement, love and support always. I am here because you first believed in me

To Uncle Gbenga, Anty Busola, and Ewaogo, words are not enough to thank you for being my home away from home. I am forever grateful for your prayers, love, and support. To my friends, John, Orevaoghene, Fama, Francisca, David, Abraham, Keturah, and Sarah, near and far, you never cease to listen to me and shower me with support and encouragement. You all make me a better person. Thank you all for being there.

OUTPUTS FROM THIS WORK

Publication Arising from Research:

Mol, B.A., **Wasinda, J.J**., Xu, Yi F., Gentle, N.L and Meyer, V. (2024) 1,25-dihydroxyvitamin D_3 augments low-dose PMA-based monocyte-to-macrophage differentiation in THP-1 cells, Journal of Immunological Methods, 532, p. 113716, doi: org/10.1016/j.jim.2024.113716.

Presentation Arising from Research:

Wasinda, J.J., Gentle, N.L and Meyer, V. Differentiation with 1,25-Dihydroxyvitamin D_3 Enhances Macrophage Polarisation and Function in THP-1 Cells. Molecular Biosciences Research Thrust (MBRT) Research Symposium, University of the Witwatersrand (5 December 2024). Poster presentation by Wasinda J.

TABLE OF CONTENTS

LIST OF FIGURES

LIST OF TABLES

LIST OF ABBREVIATIONS

$1,25D_3$	1,25-Dihydroxyvitamin D_3
$25D_3$	25-Hydroxyvitamin D
5'ppp-dsRNA	5' Triphosphate double-stranded RNA
ALOX15	Arachidonate 15-lipoxygenase
ANOVA	Analysis of variance
CD80	Cluster of differentiation 80
cDNA	Complementary DNA
CCL-2	C-C motif chemokine ligand 2
CXCL-10	C-X-C motif chemokine ligand 10
CYP27B1	1α-Hydroxylase
CYP27A1	Sterol 27-hydroxylase
CYP2R1	25-hydroxylase
FBS	Foetal bovine serum
IFN	Interferon
IFN-γ	Interferon-gamma
IL-1β	Interleukin -1 beta
iNOS	Inducible nitric oxide synthase
ISGs	Interferon-stimulated genes
IκBα	Kappa B alpha
LPS	Lipopolysaccharides
M0	Naïve macrophage
M1	Classically activated macrophage
M2	Alternatively activated macrophage

MHC II	Major histocompatibility complex II
NF-κB	Nuclear factor-kappa B
NO	Nitric oxide
NLRs	Nucleotide oligomerisation domain-like receptors
PAMPs	Pathogen-associated molecular patterns
PBS	Phosphate-buffered saline
PKC	Protein kinase C
PMA	Phorbol-12-myristate-13-acetate
PRR	Pattern recognition receptors
P/S	Penicillin-streptomycin
RA	Rheumatoid arthritis
RIG-I	Retinoic acid-inducible gene I
RLRs	Retinoic acid-inducible gene I (RIG-I)-like receptors
RNA Seq	RNA sequencing
ROS	Reactive oxygen species
RPMI	Roswell Park Memorial Institute 1640 medium
RT-qPCR	Reverse transcriptase quantitative polymerase chain reaction
RXR	Retinoid X receptor
TLR	Toll-Like receptors
TNF-α	Tumour necrosis factor-alpha
TH-2	T-helper 2
UBC	Ubiquitin C
UVB	Ultraviolet B radiation
VDBP	Vitamin D binding protein

VDR	Vitamin D receptor
VDREs	Vitamin D response elements
YWHAZ	Tyrosine 3-monooxygenase/tryptophan 5-monooxygenase activation protein zeta

ABSTRACT

Macrophages are innate immune cells, leading the early defence against invading pathogens. The highly versatile and adaptable nature of macrophages is critical in maintaining immune homeostasis. The dysregulation of macrophage function has been linked to various pathologies. Hence, understanding macrophage biology is essential. THP-1 cells are the most widely used *in vitro* model for studying macrophage biology. Despite its broad adoption, the experimental protocol for obtaining mature macrophages from THP-1 cells has not been standardised. This is particularly evident when it comes to the concentration of phorbol 12-myristate 13-acetate (PMA), a widely used differentiation agent, and its associated impact on the inflammatory state of the derived macrophages. 1,25-Dihydroxyvitamin D_3 ($1,25D_3$), a well-known immunomodulator with anti-inflammatory properties, has the potential to augment the limitations of PMA-based differentiation protocols. This study, therefore, hypothesised that a low-dose PMA-based differentiation protocol in the presence of $1,25D_3$ would yield functional, naive macrophages (M0) that can be polarised into either the pro-inflammatory (M1) or anti-inflammatory (M2) phenotype. To test this premise, THP-1 cells were differentiated with 5 nM PMA, in the presence and absence of 10 nM $1,25D_3$. To evaluate the functional implication of the differentiation protocol on their polarisation potential, M0 macrophages were stimulated for 24 h with 100 ng/ml lipopolysaccharide (LPS) and 20 ng/ml of interferon-Gamma (IFN-γ) to obtain M1 macrophages or 20 ng/ml interleukin 4 (IL-4) and 20 ng/ml IL-13 for 48 h to obtain M2 macrophages. The surface expression of M1-marker, CD80, and M2-marker, CD206, were then quantified by flow cytometry. As further confirmation of the inflammatory state of the cells, the expression levels of key inflammatory markers (*RIG-I, IL-1β, CXCL-10, CCL-2 and IL-10*) were quantified using RT-qPCR. To test the functional potential of the macrophages, they were transfected with the retinoic acid-inducible gene I (RIG-I) agonist, 5'ppp-dsRNA, for 2 h. The results revealed that the presence of $1,25D_3$ caused differentiated cells to adopt a morphology comparable to primary macrophages. Differentiation in the presence of $1,25D_3$ also supported macrophage polarisation into distinct M1 and M2 phenotypes based on CD80 and CD206 expression in response to IFN-γ + LPS and IL-4 + IL-13, respectively. Moreover, M1 macrophages differentiated from M0 macrophages obtained in the presence $1,25D_3$ showed significantly higher expression of inflammatory markers *RIG-I* and *CXCL-10*, compared to M1 macrophages differentiated from M0 macrophages in the absence of $1,25D_3$. Regardless of $1,25D_3$ presence during differentiation, neither M0 nor M1 macrophages launched a notable response to 5'ppp-dsRNA 2 hours post-transfection. However,

M2 macrophages differentiated from M0 macrophages in the presence of $1,25D_3$ responded with a significant increase in inflammatory markers *CXCL-10* ($p < 0.001$) and *CCL-2* ($p < 0.050$) relative to the control. Thus, the presence of $1,25D_3$ during differentiation appears to support a macrophage phenotype that can respond to both inflammatory and anti-inflammatory signals. Taken together, the results support the premise that $1,25D_3$ augments low-dose PMA-based differentiation of THP-1 cells into functional macrophages.

CHAPTER 1: LITERATURE REVIEW

1.1 Macrophages

1.1.1 Macrophage origin and function

Macrophages are innate immune cells and key players in the first line of defence against pathogens, including viruses, bacteria (Hirayama et al., 2018). They exist as tissue-resident cells developed during the early embryonic developmental stage with self-renewal ability (Epelman et al., 2014). They can equally be differentiated from circulating monocytes - a myeloid progenitor cell integral in the maintenance of endothelial integrity as demonstrated in Fig 1.1 (Auffray et al., 2009; Teh et al., 2019; Lendeckel et al., 2022). Tissue-resident macrophages such as Kupffer, alveolar, microglia, and osteoclast cells found in the liver, lungs, brain, and bone, respectively, are shaped uniquely to their location. Irrespective of their origin, tissue-resident and monocyte-derived macrophages migrate to the affected area and function in combination to clear pathogens (Galli et al., 2011; Davies et al., 2013; Lendeckel et al., 2022).

Chemotactic signalling directs tissue-resident and recruited monocyte-derived macrophages to the site of injury or infection, and this is usually associated with inflammation. Through phagocytosis (Fig. 1.1), macrophages engulf invading pathogens and other cell debris. Phagocytosed pathogens are broken down after isolation in the phagosome, fusion with lysosomes and formation of a phagolysosome (Hirayama et al., 2018). Antigen-presentation follows when peptide residues from phagocytosis, usually consisting of 15 - 20 amino acids, are carried over and presented to the adaptive immune T cells via the major histocompatibility complex II (MHC II) cell surface molecule (Roche and Furuta, 2015; Santa, 2023).

Pathogenic invasion of the host cellular environment is picked up by the close monitoring activity of pattern recognition receptors (PRR) (Fig. 1.1). This signals the activation of macrophages and other innate immune cells through the identification and binding to pathogen-associated molecular patterns (PAMPs) exhibited by the pathogens. PRRs are found within the extra and intracellular spaces of innate immune cells such as macrophages, neutrophils, and dendritic cells. Major examples include the toll-like receptors (TLR), nucleotide oligomerisation domain-like receptors (NLRs) and retinoic acid-inducible gene I (RIG-I)-like receptors (RLRs) (Kumar et al., 2011; Rehwinkel and Gack, 2020). Activating PRRs such as RIG-I for example, by short, double-stranded RNAs with a 5' triphosphate and blunt ends, results in a robust signalling cascade via the nuclear factor-kappa B (NF-κB) signalling

pathway. This results in the release of pro-inflammatory cytokines such as tumour necrosis factor-alpha (TNF-α), interleukin-1 beta (IL-1β), IL-8, IL-6 and IL-12. At the same time, chemokines such as C-X-C motif chemokine ligand 10 (CXCL-10) and C-C motif chemokine ligand 2 (CCL-2) are released. They work together to cause an increased vascular permeability enabling the recruitment of other inflammatory cells. Concurrently, via the interferon regulatory factors (IRF) signalling pathway, a type I interferon (IFN) response is also activated. This leads to the transcription of interferon-stimulated genes (ISGs) inducing an antiviral state in infected cells extending to neighbouring cells (Duque and Descoteaux, 2014; Lendeckel et al., 2022).

In vitro, these immune signalling pathways can be activated by means of synthetic agonists for the PRRs. Commonly used agonists to stimulate an antiviral response include for example, resiquimod (TLR7/8 agonist; Miller et al., 2008; Frega et al., 2020) and 5'ppp-dsRNA (RIG-I agonist; Goulet et al., 2013), while antibacterial responses can be induced by LPS (TLR4 agonist; Tan and Kagan, 2014) and Pam_3CysSK_4 (TLR2/1 agonist; Du et al., 2019).

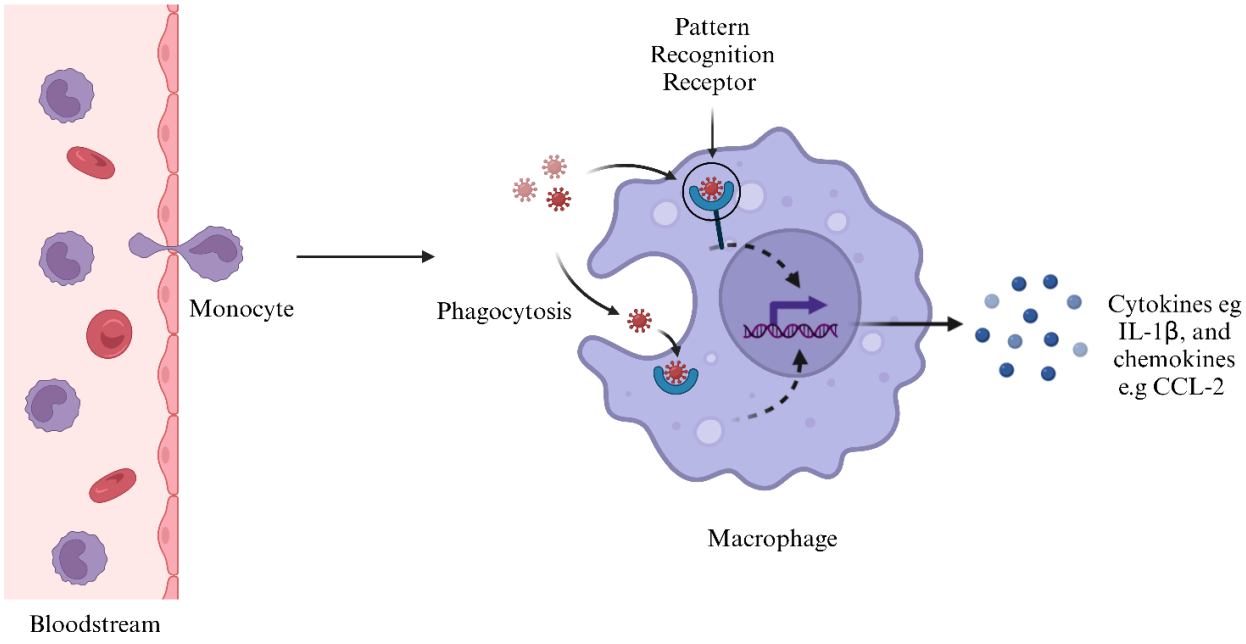

Figure 1.1: Monocyte-to-macrophage differentiation. Circulating monocytes leave the bloodstream and enter tissues in response to changes in environmental cues. In tissues, monocytes differentiate into macrophages and phagocytose pathogens. Macrophages possess pattern recognition receptors (PRRs) that recognise pathogen-associated molecular patterns (PAMPs) exhibited by invading pathogens. PAMP recognition results in a signalling cascade leading to the production and release of pro-inflammatory cytokines such as IL-1β and chemokines such as CCL-2. (Images created on Biorender.com)

1.1.2 Macrophage polarisation

Macrophages are highly adaptable cells, critical in the maintenance of homeostasis. Influenced by their surroundings, macrophages exhibit heterogeneity and can assume distinct physical characteristics and immunological functions through a process referred to as polarisation. Resting, naïve or simply M0 macrophages, when activated, can polarise into either classical (M1) or alternative (M2) phenotypes. M1 and M2 macrophages are associated with pro-inflammatory and anti-inflammatory environments, respectively (Lendeckel et al., 2022). Xue et al. (2014) argue that the M1 and M2 classification of macrophages is too simplistic. They describe the polarisation of macrophages as a wide spectrum, with M1 and M2 macrophages representing only the opposite ends (Locati et al., 2020). Macrophage diversity is largely a result of signals from environmental stimuli, determined by cytokine release, inflammation, and pathogen-associated molecules such as lipopolysaccharides (LPS) and fatty acids (Lampiasi et al., 2016; Hirayama et al., 2018).

Macrophages assume an M1 phenotype during pathogenic invasion, activated usually by exposure to microbial products and cytokines such as LPS and interferon-gamma (IFN-γ), respectively. Arginine metabolism is downregulated in M1 macrophages to enable the inducible nitric oxide synthase (iNOS) pathway, which ensures the production of nitric oxide (NO) for an antimicrobial response (Weisser et al., 2013; Lampiasi et al., 2016). M1 macrophages express the co-stimulatory protein surface markers, cluster of differentiation (CD) 80 and CD78, and the MHC class II proteins. CD80 plays an important role in the activation and proliferation of T cells, a key step in furthering the immune response against pathogens and supporting the inflammatory state (Orlikowsky et al., 1999; Parker, 2018). Activated M1 macrophages proceed to exert a robust inflammatory response marked by the high production and release of pro-inflammatory cytokines such as TNF-α, IL-6, and IL-1β, and chemokines such as CXCL-10, and CXCL-9, as shown in Fig. 1.2 (Shapouri-Moghaddam et al., 2018). The production of pro-inflammatory cytokines and chemokines causes positive feedback, recruiting naïve macrophage (M0) into the M1 phenotype and to the infection site. This is also accompanied by the production of NO and reactive oxygen species (ROS), necessary for eliminating pathogens (Xuan et al., 2015). These events are completed by the presentation of antigens to T-cells via the now actively expressed MHC class II, ushering in the adaptive immune system. The aggressive response exerted at the early stage of infection by M1 macrophages is critical in limiting the spread of pathogens. However, regulation of M1 macrophages is important to mitigate chronic inflammation, capable of causing tissue damage

and inflammatory diseases such as atherosclerosis, inflammatory bowel diseases, etc. (Weisser et al., 2013; Martinez and Gordon, 2014; Wang et al., 2014; Porta et al., 2015; Murray, 2017).

Conversely, M2 macrophages direct opposing functions to M1 macrophages. They are a product of the arginase pathways, producing ornithine and urea as by-products (Lampiasi et al., 2016). M2 macrophages facilitate the resolution of inflammation, leading the cells into wound healing, tissue repair and regeneration by producing anti-inflammatory cytokines such as IL-10, resolving the inflammation and cytotoxic environment created by M1 macrophages. In addition, they produce factors that facilitate angiogenesis and purging of apoptotic cells as captured in Fig. 1.2. (O'Shea and Paul, 2010; Wang et al., 2014; Porta et al., 2015). M2 macrophages are typically stimulated by the downstream signalling of cytokines such as IL-13 and IL-4 (Van Dyken and Locksley, 2013; Scott et al., 2023). High expression of surface markers such as the mannose receptor CD206, alongside CD163 and CD209, mark M2 macrophages (Gordon and Martinez, 2010; Wang et al., 2014). CD206 plays a multifunctional role in M2 macrophages, including anti-inflammatory tissue repair functions, and pattern recognition (Wynn and Vannella, 2016; Sadtler et al., 2023). Prolonged induction of M2 macrophages can be detrimental, where scarring due to excessive tissue repair leads to organ failure. Even worse, the immunosuppressive microenvironment is capable of promoting the diversion of immune detection by cancerous cells, enabling tumour growth and metastasis (Zhou et al., 2015; Wang et al., 2019).

M2 macrophages can be further sub-classified into M2a, M2b, M2c and M2d, each expressing unique characteristics and functions (Yao et al., 2019). Their functions vary from the enhancement of endocytic activity, tissue repair, regulation of the immune response and the promotion of tumour progression, respectively (Zizzo et al., 2012; Ferrante et al., 2013; Wang et al., 2019; Yao et al., 2019). The polarisation of macrophages is not permanent as it can reverse or assume a new phenotype, exerting a different function (Fig. 1.2). This phenomenon, facilitated by the changing microenvironment, is vital in maintaining homeostasis (Peng et al., 2023).

Maintaining an equilibrium between the M1 and M2 macrophage polarisation states is instrumental for not just homeostasis but for overall health outcomes, as disruption has been linked to autoimmune diseases, among others (Wang et al., 2014). Prolonged activation of M1 promotes further inflammation with detrimental impact. Similarly, aberrant activation of M2

macrophages caused by oestrogen and progesterone has also been linked to the prevalence of autoimmune diseases in women (Routley and Ashcroft, 2009; Menzies et al., 2011; Funes et al., 2018). In cancer, M1 macrophages are associated with the promotion of attack towards tumours, while activation of M2 macrophages promotes tumour growth. As part of intervention strategies, many recent therapies are exploring targeting the ablation of excessive M1 macrophages in hyper-inflammatory environments to bring balance. This new strategy will achieve this by the selective marking and taking out of specific subpopulations of macrophages needed to restore M1/M2 balance (Gabrilovich et al., 2012).

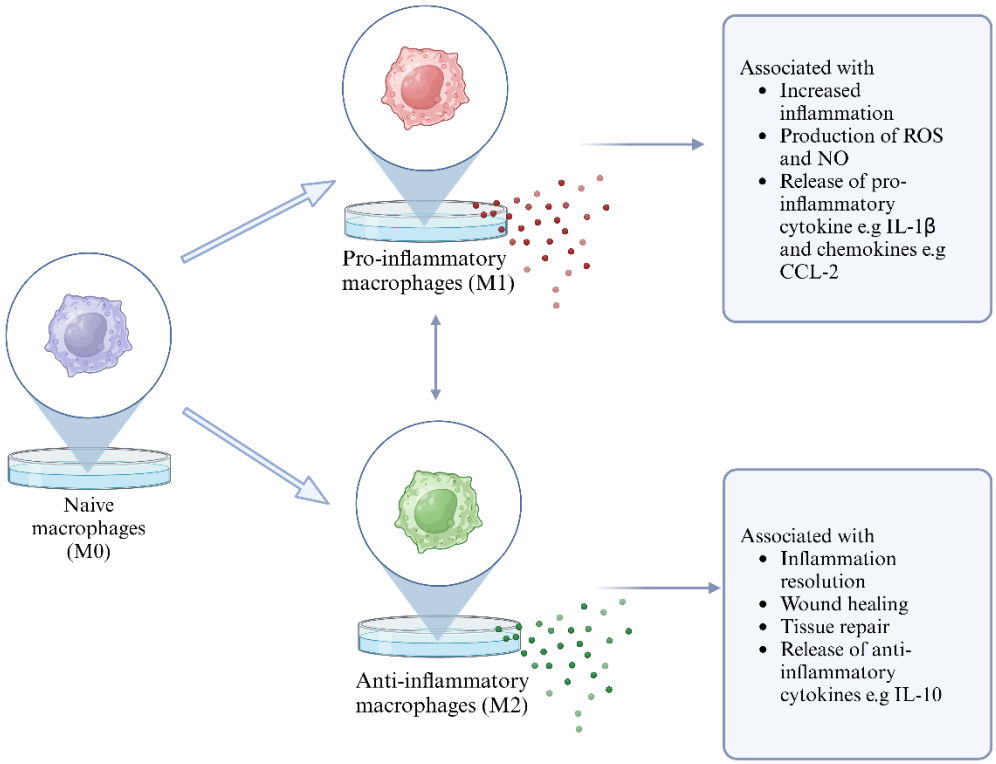

Figure 1.2: Macrophage polarisation into the M1 and M2 states. Naïve (M0) macrophages, in response to changes in environment, polarise into M1 or M2 macrophages. M1 macrophages are associated with inflammation, producing and releasing pro-inflammatory cytokines such as IL-1β and chemokines such as CCL-2. Anti-inflammatory M2 macrophages mediate the resolution of the inflammatory state, also leading to wound healing, and tissue repair, in addition to producing and releasing anti-inflammatory cytokines. (Images created on Biorender.com)

1.2 Vitamin D

1.2.1 Vitamin D origin and metabolism

Vitamin D is a fat-soluble hormone principal in the absorption of vital minerals such as calcium and phosphate, with musculoskeletal functions including bone remodelling and maintaining

bone strength (Bell et al., 2010; Snegarova and Naydenova, 2020). Collectively referred to as vitamin D, and as captured in Fig. 1.3, cholecalciferol and ergocalciferol represent its two main classes. Cholecalciferol originates from the photochemical conversion of 7-dehydrocholesterol embedded in the epidermis of the skin of animals as a result of exposure to ultraviolet B radiation (UVB; ~300 – 325 nm) - the main source of vitamin D (White, 2012). Alternatively, cholecalciferol can be obtained from animal products with the flesh of fatty fish and fish liver oils leading as rich sources. On the other hand, ergocalciferols are obtained primarily from dietary sources, mostly occurring in mushrooms and more commonly vitamin D-fortified foods (Colotta et al., 2017).

Regardless of origin, vitamin D is subjected to a two-step modification, converting it into a biologically useful compound (Fig. 1.3). It undergoes hydroxylation in the liver, a process that converts vitamin D into 25-hydroxyvitamin D_3 ($25D_3$; calcidiol) by the cytochrome P450 25-hydroxylase enzymes CYP27A1 and CYP2R1 (Zhu and Deluca, 2012; Christakos et al., 2016). $25D_3$ represents the most occurring and storage form of vitamin D in animals used as a matrix for assessing vitamin D status in the body system (Heaney et al., 2009). In the next stage, 25-hydroxyvitamin D is further converted into its biologically active form 1,25- dihydroxy vitamin D_3 ($1,25D_3$; calcitriol) by 1α hydroxylase enzyme (CYP27B1) in the kidneys and released into circulation. $25D_3$ and $1,25D_3$ are both conveyed around the bloodstream bound to the vitamin D binding protein (VDBP; White, 2012; Christakos et al., 2016).

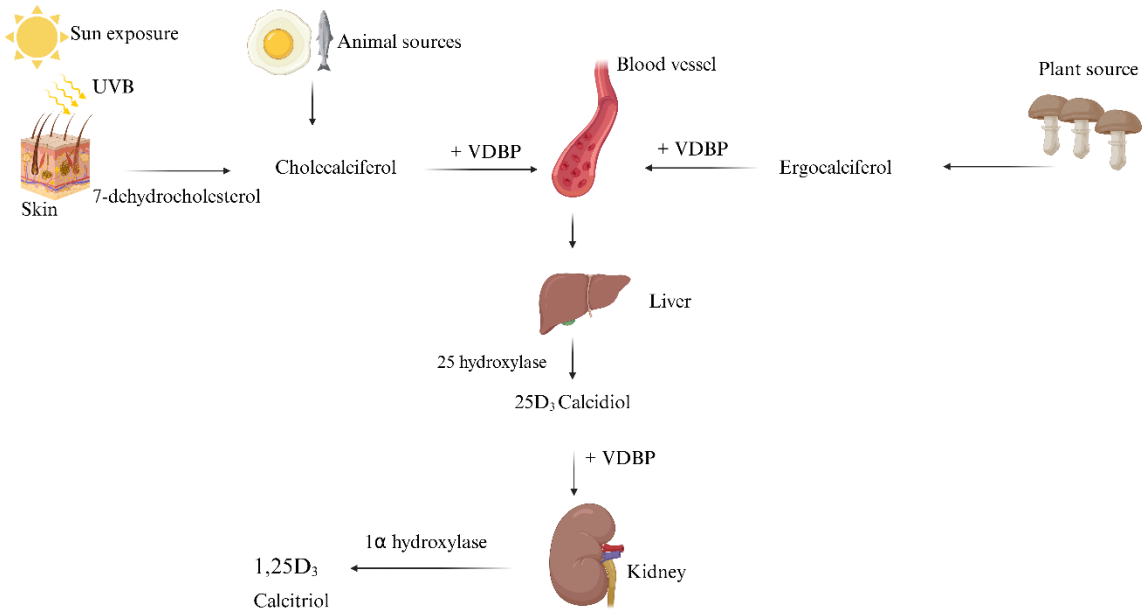

Figure 1.3: Obtaining biologically active vitamin D. Upon exposure to sunlight, the skin absorbs ultraviolet B radiation (UVB), which converts 7-dehydrocholesterol into cholecalciferol also obtainable from animal sources such as fatty fish. Alongside ergocalciferol, obtainable from plant sources such as mushrooms, cholecalciferol is further transported through the bloodstream bound to the vitamin D binding proteins (VDBP) into the liver where they are converted into $25D_3$ (25-hydroxyvitamin D_3; calcidiol) in the presence of 25-hydroxylase enzyme. Also bound to the VDBP, $25D_3$ is transported to the kidney and converted into $1,25D_3$ (1,25-dihydroxyvitamin D_3; calcitriol) in the presence of 1 α hydroxylase enzyme. (Images created on Biorender.com).

1.2.2 The Vitamin D receptor and immunomodulatory function in macrophages and immunity

A fundamental change in the understanding of the physiological activity of vitamin D began upon the discovery of the extra-renal presence of CYP27B1 and the vitamin D receptor (VDR; Lang et al., 2013). VDR belongs to a family of nuclear hormone receptors made up of conserved DNA and α-helical binding domains, which upon activation function as a transcription factor. In the presence of vitamin D, delivered by the VDBP from blood circulation, the VDR is activated through a ligand-receptor interaction. Activated VDR proceeds to form a heterodimer with a retinoid x receptor (RXR), which is necessary for binding to vitamin D response elements (VDREs) found in the promoter regions of vitamin D target genes - enabling gene transcription or inhibition and captured in fig. 1.4 (White, 2012; Colotta et al., 2017).

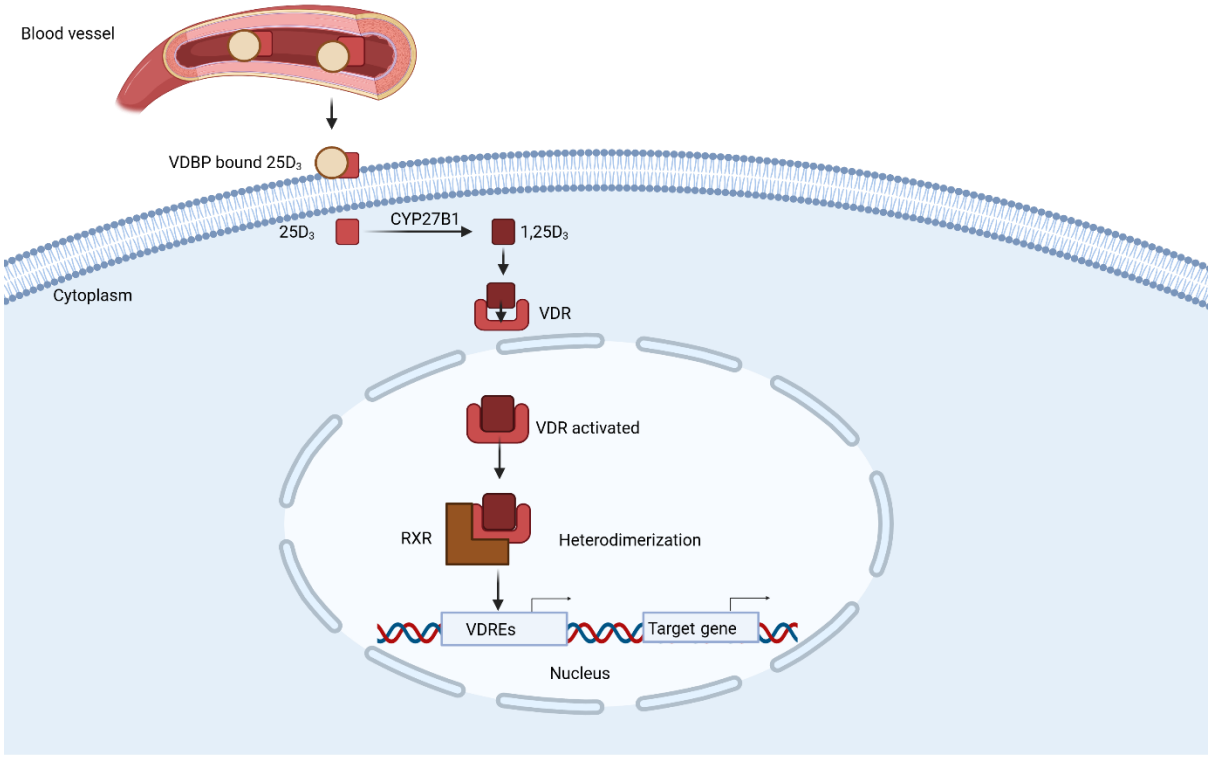

Figure 1.4: Activation of the vitamin D receptor. The $25D_3$ from blood circulation enters the cell transported by the vitamin D binding protein (VDBP). The delivered $25D_3$ is converted into $1,25D_3$ by the 1-alpha-hydroxylase (CYP27B1) enzyme and proceeds to bind to the vitamin D receptor (VDR), resulting in a conformational change and activation. Activated VDR forms a heterodimer with a retinoid X receptor (RXR), which binds to DNA sequences called the vitamin D response element (VDREs), leading to the transcription of target genes. (Images created on Biorender.com)

The local presence of VDR, particularly in innate immune cells such as activated dendritic cells and macrophages suggests its strong physiological roles indicating $1,25D_3$ as an endogenous immune modulator (Bishop et al., 2021). During pathogen recognition by PRRs and phagocytosis in monocytes, CYP27B1 activity was reported to be elevated, indicating an increase in the endogenous production of biologically active $1,25D_3$ (Esteban et al., 2004). This could be a result of the capacity of immune cells to convert 25D to $1,25D_3$ inducing paracrine and autocrine production of $1,25D_3$ (Krutzik et al., 2008).

The immunomodulatory function of $1,25D_3$ is inclusive of the promotion of cell differentiation, inhibition of cell proliferation and the release of antimicrobial proteins such as cathelicidin (Kamen and Tangpricha, 2010; Sanlier and Guney-Coskun, 2022). Most importantly it functions in the attenuation of a vigorous pro-inflammatory response, and the inhibition of pro-inflammatory cytokines such as IL-6 and IL-8. Additionally, it increases the prevalence of anti-inflammatory cytokines such as IL-4 and IL-10 through the activation of the T-helper 2 (Th 2) cells and inhibition of the Th1 and Th17 cells (Sanlier and Guney-Coskun, 2022). One

of the known mechanisms by which $1,25D_3$ regulates cytokine production is through the upregulation of the protein, Inhibitor of kappa B alpha (IκBα), inhibiting NF-κB-mediated p65 activation (Chen et al., 2013; Colotta et al., 2017). $1,25D_3$ has also been reported to be involved in the regulation of CD4+ T cell function (Mehta et al., 2010), in addition to several other studies reporting evidence of $1,25D_3$ immune modulation in innate immune cells (Cutolo, 2008; Zhang et al., 2012; Tian et al., 2016; Jadhav et al., 2018; Zhao et al., 2020).

The association of $1,25D_3$ deficiency and the susceptibility and/or exacerbation of certain diseases have been suggested in multiple studies. A classic example is the relationship between the prevalence of diseases such as respiratory infection and varying $1,25D_3$ levels during certain seasons (Cannell et al., 2006; Siddiqui et al., 2020). Additionally, the trigger and progression of some cardiovascular and autoimmune diseases such as rheumatoid arthritis (RA) have also been linked to the deficiency of $1,25D_3$ (de la Torre Lossa et al., 2020). The biological availability of $1,25D_3$ via supplementation was suggested to protect against viral infection. Meanwhile, many studies equally disproved this claim by demonstrating the lack of correlation and the inability to establish dosage (Chadha et al., 2011; Gui et al., 2017; Lin et al., 2017; Loeb et al., 2019).

$1,25D_3$ has long been a potential agent for monocyte-to-macrophage differentiation (Schwende et al., 1996). Studies have reported that during monocyte-to-macrophage differentiation, $1,25D_3$ interaction with VDR initiates transcriptional changes that support differentiation (Schwende et al., 1996; Daigneault et al., 2010; Rynikova et al., 2023). $1,25D_3$ supplementation has been reported to enhance cell adherence and support differentiation by actively taking part in regulating the expression of adhesion molecules and cytoskeletal proteins (Oghogho Omage et al., 2024). Often referred to as a physiological agent for macrophage differentiation (Svetlana et al., 2018), $1,25D_3$ has also been reported to elevate the expression of CD14, CD11b and CD36, which primes monocytes for differentiation (Adams and Hewison, 2008; Van den Bossche et al., 2017).

1.3 THP-1 Cell line: *In vitro* model for studying macrophages

1.3.1 THP-1 origin and function

Amongst the multiple ways to study macrophages *in vitro*, it is logical to assume that the most accurate approach would be through their isolation from the tissue of interest. This approach, however, requires a considerable amount of blood obtainable through donations or other invasive methods such as biopsy of the target tissue (Jensen et al., 2021; Rynikova et al., 2023).

Regardless of the isolation procedure, macrophages isolated from tissue are usually present in low amounts, with low proliferation capacity (Daigneault et al., 2010). Hence, immortalised cell lines have become a more suitable alternative model for studying macrophage biology, with well-known examples such as THP-1, U937 and HL-60 (Rynikova et al., 2023).

Since the first successful establishment in 1951, human-derived cell lines have been instrumental in research developments such as advancing vaccine development, cancer and genetic research, better understanding of drug mechanisms etc. (Sarntivijai et al., 2014) THP-1 is a promonocytic cell line, isolated from the peripheral blood of a 1-year-old acute monocytic leukaemia patient and was first established by Tsuchiya et al. (1980). It is a widely used model for studying monocyte and macrophage biology for its homogeneity, ease of maintenance, proliferation, and ability to respond to various stimuli through monocyte signalling pathways (Baxter et al., 2020). The ability to store THP-1 cells indefinitely in liquid nitrogen without an impact on cell viability and biology adds a point to its preference, especially when compared to primary macrophages that come with the challenge of accessibility, variability from donors and a high chance of contamination with other cells. THP-1 cells differentiate into macrophage-like cells with morphology characteristics mimicking human primary macrophages and are thus used extensively in studying the function, signalling patterns and pathways, and the functional implications of macrophage polarisation (Qin, 2012; Chanput et al., 2014).

1.3.2 THP-1 differentiation protocol and experimental outcomes

The convenience of using cell lines such as THP-1 for macrophage studies also comes with setbacks. Results obtained may fail to accurately represent primary tissue macrophages. Many protocols for THP-1 macrophage differentiation have been developed over the years, each attempting to produce macrophages with the best comparison to primary macrophages in morphology, physiological and pathological characteristics and function (Daigneault et al., 2010; Murray, 2017). Several differentiation agents have been reported to be used to obtain macrophages. Examples include retinoic acid, $1,25D_3$, cytokines e.g. TNF-α and IFN-γ; and the most reported, phorbol-12-myristate-13-acetate (PMA; Schwende et al., 1996; Chen and Ross, 2004; Humeniuk-Polaczek and Marcinkowska, 2004).

Introducing PMA to the well-rounded single suspended THP-1 cells causes them to adopt a highly adherent nature, as an initial stage of the monocyte-to-macrophage differentiation. PMA is a phorbol ester that mimics a diacylglycerol (DAG) and activates protein kinase C (PKC) by binding to its C1 domain. Activated PKC initiates intracellular signalling pathways such as the

NF-κB signalling pathway causing changes in gene expression leading to morphological and functional shifts (Liu and Heckman, 1998). Complete differentiation is defined by the morphological transformation of THP-1 cells into a flat, amoeboid-shaped macrophage with reduced proliferation, increased rate of phagocytosis and surface expression of CD11b and CD14 (Schwende et al., 1996; Qin, 2012).

Various concentrations of PMA have been used in different studies to obtain macrophages *in vitro* (Table 1). These concentrations varied from as low as 6 nM to as high as 500 nM with incubation times in culture medium ranging from 3 to 72 h followed by varying resting periods in some studies. Most of the high PMA concentration protocols reported cell adherence and the assumption of a macrophage-like morphology (Park et al., 2007; Daigneault et al., 2010; Spano et al., 2013; Tulk et al., 2015; Lund et al., 2016). However, it was also reported in multiple studies that the macrophages obtained went straight into an M1-activated phenotypic state, as seen by the aberrant expression of inflammatory markers amongst genes at baseline. The expression of these inflammatory markers was directly proportional to the increase in the concentration of PMA used (Maeß et al., 2014; Lund et al., 2016). This proved to be problematic as the baseline expression of inflammatory markers, amongst others, can mask the true biological outcomes of the investigation at hand. For example, such a baseline-activated state may overshadow any small expression changes expected from an applied stimulus in culture (Park et al., 2007; Lund et al., 2016).

In an attempt to circumvent the problem, lower concentrations of PMA have been explored by more recent studies in a dose-dependent manner. In their study, Park et al. (2007) reported that 5 ng/ml PMA was sufficient to cause stable THP-1 differentiation into macrophages without the baseline expression of inflammatory markers previously recorded at 25 - 100 ng/ml PMA concentrations. The macrophages obtained were reported to be responsive to low-concentration stimuli. Conversely, other studies have reported that the use of lower PMA concentrations (6 nM and 30 nM) led to a partial restoration of proliferative activity. In other words, a de-differentiation was observed with (Spano et al., 2013) or without (Lund et al., 2016) the withdrawal of PMA from the culture medium. In addition to the baseline inflammatory state reported following differentiation with higher concentrations of PMA, the macrophage priming impacts the distinct polarisation into an M2 phenotypic state. Macrophages differentiated with high PMA concentration failed to upregulate markers of M2 macrophages such as C-C Motif Chemokine ligand 17 (CCL17) and Arachidonate 15-lipoxygenase (ALOX15) after polarisation (Baxter et al., 2020; Chanput et al., 2014).

Additionally, time in culture and subsequent rest periods in a PMA-free medium were all factors that were said to influence THP-1 differentiation and the subsequent polarisation process (Aldo et al., 2013; Starr et al., 2018). Baxter et al. (2020) reported that a 72-h resting period in fresh medium following 24 h in culture with PMA may result in the reduction of interferon regulatory factor 1 (IRF 1) and signal transducer and activator of transcription 1 (STAT1) expression, which enables polarisation into an M2 phenotype. This was, however, not the case when cells were rested in a PMA-free medium for just 24 h.

Despite being the most widely used cell line for macrophage study *in vitro*, there is no agreed-upon standard for the THP-1 macrophage differentiation protocol. *In vitro* studies are an essential part of the initial stages of biological research, reflecting an *in vivo* environment. It is an important stage in the attempts to understand the physiology, pathology, overall behavioural characteristics of biological phenomena, and response to treatment of any kind. For this reason, the development and utilisation of the most applicable experimental protocol in a biological condition needs to be adopted. The inconsistencies and inability to reproduce results due to differing THP-1 differentiation protocols reported in multiple studies over time need to be standardised.

Table 1: Effect of PMA concentration on THP-1 macrophage differentiation outcome

PMA concentration	Culture time (h)	Rest period (h)	Confirmatory method	Outcome	Reference
8 nM 25 nM 50 nM 100 nM 200 nM	48	0 – 120	qPCR Flow cytometry	● TNF-α expression was elevated with increasing PMA concentration without additional stimulation. ● After LPS stimulation, TNF-α expression was directly proportional to the increasing PMA concentration. ● Regardless of rest period, 8 - 25 nM PMA responded similarly to weak and strong LPS stimulation. ● Weak LPS stimulation was masked in cells differentiated with 50 nM and above.	(Lund et al., 2016)
200 ng/ml	24 48	- -	Flow cytometry	● CD11b and CD14 had the lowest expression in THP-1 differentiated for a day compared to cells differentiated for 5 days.	(Starr et al., 2018)
6 nM 30 nM 60 nM	72	-	Flow cytometry	● Cell adherence was increased with an increase in PMA concentration ● 30 nM of PMA caused an intermediary level of differentiation having a heterogeneous population ● Withdrawal of PMA after 72h in culture caused detachment of cells, apoptosis and interesting appearance of a dendritic cell-like morphology	(Spano et al., 2007)
30 nM 100 nM	24 48	- 24	qPCR Flow cytometry	● 30 nM PMA cause differentiation into immature macrophages with no full adherence and retainment of spherical shape ● 100 nM gave mature macrophages that were adherent with flat microvilli projections	(McCartan et al., 2015)

Table 1: Effect of PMA concentration on THP-1 macrophage differentiation outcome continued

PMA concentration	Culture time (h)	Rest period (h)	Confirmatory method	Outcome	Reference
15 nM	24	24	qPCR	● Differentiated macrophages showed adherence and a decrease in proliferation. ● They also expressed JAK-STAT1 signature genes.	(Melbourne et al., 2020)
50 ng/ml	72	24	qPCR Flow cytometry	● Differentiated macrophages showed a decrease in monocyte surface marker CD14 and an increase in macrophage surface markers CD11b, CD11c and CD86.	(Rojas et al., 2016)
50 ng/ml	48	72	qPCR Flow cytometry	● Differentiated macrophages formed a heterogenous population having both round and spindle-shaped cells	(Shiratori et al., 2017)
10 nM	72	72	qPCR Flow cytometry	● 99.5% of differentiated macrophages had CD11b surface marker expression ● Differentiated macrophages were responsive to M1 and M2 activation.	(Suski et al., 2020)
10 ng/ml	24	48	qPCR Flow cytometry	● PMA treatment caused cell adherence with a flat and amoeboid shape presentation ● M1 and M2 macrophages obtained expression of CXCL-10 and CD206 respectively.	(Morón-Calvente et al., 2018)

1.4 Study rationale and hypothesis

So far, PMA is arguably the most reliable option for THP-1 differentiation. Hence, PMA-based protocols must be optimised and standardised. This can be achieved by exploring possible ways of mitigating its limitations and augmenting its capacity to cause differentiation. One such method was explored by (Valdés López and Urcuqui-Inchima, (2018), who studied the potential of combining low-dose PMA with $1,25D_3$ to cause differentiation in the U937 cell line. $1,25D_3$ as a sole differentiation agent only caused minimal expression of CD11b and CD14 and failed to induce the morphology characteristics associated with mature macrophages (Daigneault et al., 2010; Rynikova et al., 2023; Mol et al., 2024). Nevertheless, its capacity to manage inflammation amongst other immunomodulatory functions captured earlier indicates its propensity to enhance a low-concentration PMA-based differentiation of THP-1 cells to obtain macrophages closely related to primary macrophages in morphology, physiology and response to treatment. We, therefore, hypothesised that a low-dose PMA-based differentiation protocol in the presence of $1,25D_3$ would yield functional, naive macrophages (M0) that could be polarised into either the pro-inflammatory (M1) or anti-inflammatory (M2) phenotype.

1.5 Aim

The aim of this study was thus to evaluate the impact of $1,25D_3$ on low-dose PMA-based THP-1 monocyte-to-macrophage differentiation, polarisation and functional potential.

1.6 Objectives

To achieve the aim, the following objectives were followed:

1. To differentiate promonocytic THP-1 cells into M0 macrophages
2. To polarise M0 macrophages into M1 and M2 phenotypes
3. To activate M0, M1 and M2 macrophages, through the PRR, RIG-I, in the presence and absence of $1,25D_3$
4. To quantify gene expression of the inflammatory markers *RIG-I*, *IL-1β*, *IL-10*, *CXCL-10*, and *CCL-2*.

CHAPTER 2: METHODOLOGY

2.1 THP-1 cell revival, culture and maintenance

To study the impact of $1,25D_3$ during PMA-based differentiation on macrophage polarisation and function, THP-1 cells were used as a model due to their functional versatility in macrophage studies. One million cryopreserved cells of the human monocytic THP-1 cell line (Passage 23) gifted to the laboratory by Dr H Ranchod were revived in 5 ml Roswell Park Memorial Institute 1640 medium (RPMI; Pan Biotech Aidenbach, Germany) supplemented with 20% (v/v) foetal bovine serum (FBS; Pan Biotech) and 1% (v/v) penicillin-streptomycin (p/s) cocktail (Sigma Aldrich St. Louis, Missouri). The FBS and p/s mixture provides the cells with the essential nutrients and growth factors required for cell growth, proliferation and maintenance while creating a bacterial-free environment, respectively (Ryu et al., 2017; S. Liu et al., 2023). The cells were incubated at 37 °C in 5% CO_2 in an 80% humidified incubator to about 60% confluency. Once revived and confluent, the RPMI medium was adjusted to contain 10% FBS and 1% p/s for continuous cell growth and maintenance, mirroring a more natural environment. Cell cultures were maintained at a concentration of 5×10^5 cells/ml of media. Cell viability was routinely assessed using the trypan blue exclusion assay.

2.2 Trypan blue exclusion assay

Prior to differentiation, cell viability was assessed using a trypan blue assay with the aid of a Countess II FL automated cell counter (Invitrogen, Massachusetts). The trypan blue exclusion assay is based on the principle that dead cells are unable to exclude dyes such as trypan blue, propidium and eosin, due to compromised cell membranes. Therefore, non-viable cells appeared dark, while viable cells appeared clear (Strober, 2015). The Countess II FL automated cell counter uses electrical impedance to analyse the cell images to rapidly count the cells in suspension (Vembadi et al., 2019). To perform the assay, a 1:1 ratio of cell in suspension to 1X trypan blue solution (Sigma Aldrich, St. Louis, Missouri) was loaded onto the countess haemocytometer and placed into the countess II FL automated cell counter.

2.3 Differentiating THP-1 cell line into naïve macrophages

To differentiate the THP-1 cells into naïve macrophages (M0), 3×10^6 viable THP-1 cells were plated in 60 x 15 mm culture dishes (Sigma Aldrich St. Louis, Missouri) at a concentration of 5×10^5 cells/ml per plate in 6 ml 10% FBS and 1% p/s RPMI. Cells were then treated with 5 nM PMA in the presence or absence of 10 nM $1,25D_3$. The working concentration of PMA was

prepared by first dissolving the purchased PMA (Sigma Aldrich St. Louis, Missouri) in dimethyl sulfoxide (DMSO; Sigma Aldrich St. Louis, Missouri) to a stock concentration of 1 mM. The stock solution was further diluted in tissue culture media to a concentration of 5 µM prior to use, to dilute out the DMSO. 6 µl of the 5 µM PMA working solution was added to each plate to effectively differentiate the cells with a final concentration of 5 nM PMA. Similarly, the purchased $1,25D_3$ (Sigma Aldrich St. Louis, Missouri) was first prepared by dissolving it in 100% molecular grade ethanol (Sigma Aldrich St. Louis, Missouri) to a stock concentration of 5 µM. 12 µl of the 5 µM $1,25D_3$ was added to plates designated for differentiation in the presence of $1,25D_3$ to effectively differentiate the cells in the presence of a final concentration of 10 nM $1,25D_3$. After incubation for 24 h the cell culture media was discarded, and the now adherent cells were washed with 2 ml pre-heated (37 °C) 1X phosphate-buffered saline (PBS; Tocris Biosciences, Bristol, United Kingdom) consisting of 137 mM sodium chloride, 2.7 mM potassium chloride, and 11.9 mM phosphate buffer (pH 7.5). Washed cells were then re-supplemented in 10% FBS, 1% p/s RPMI with or without 10 nM $1,25D_3$. Cells were incubated at 37 °C in 5% CO_2 in an 80% humidified incubator for a 72-hour resting period.

2.4 Microscopic confirmation of monocyte to macrophage differentiation

To confirm the differentiation of THP-1 cells into M0 macrophages, the tissue culture media was poured off and cells were washed with 2 ml pre-heated PBS at room temperature. PBS (2 ml) was added to the plates, and changes in cell morphology were visualised and captured using the EVOS FLoid Imaging System (Invitrogen, Waltham, Massachusetts) with a fixed 20X objective and 460X magnification.

2.5 Polarisation of naïve macrophages into M1 and M2 phenotypes

To obtain a polarised macrophage, following the complete 96-hour differentiation protocol, the media was replaced with fresh 10% FBS and 1% p/s RPMI and the M0 macrophages were immediately polarised into M1 or M2 macrophages. To polarise into the M1 phenotype, macrophages were treated with 100 ng/ml LPS (Sigma Aldrich St. Louis, Missouri) and 20 ng/ml of IFN-γ (Darmstadt, Germany) and incubated for 24 h (Nygaard et al., 2022). To obtain the M2 phenotype macrophages were treated with 20 ng/ml of IL-4 (Sigma Aldrich St. Louis, Missouri) and 20 ng/ml of IL-13 (Sigma Aldrich St. Louis, Missouri) in 10% FBS, 1% p/s RPMI and incubated for 48 h (Genin et al., 2015).

2.6 Cell harvesting

To confirm the polarisation state and quantify changes in gene expression, adherent macrophages had to be removed from the cell culture plates. To harvest cells, the cell culture media were poured from the plates and the plates washed with 2 ml pre-heated PBS at room temperature. The cells were then incubated in 1 ml 0.25% Trypsin-EDTA PBS for 3 min at 37 °C to detach the cells. To stop the enzymatic activity, 1 ml 10% FBS in RPMI was added, followed by gentle scraping using a cell scraper (Sigma Aldrich St. Louis, Missouri) to ensure complete removal of all the macrophages from the culture plate. The cell suspension was then subjected to centrifugation at 500 x *g* for 5 minutes at room temperature to obtain cell pellets. Cells were aliquoted and counted, and viability was assessed as described in section 2.2. The counted and aliquoted cells were either used immediately for flow cytometry, at room temperature, or snap-frozen in liquid nitrogen and stored for RNA extraction.

2.7 Flow cytometry

To confirm polarisation, the expression of the M1 and M2 macrophage surface markers, CD80 and CD206, respectively, was quantified using flow cytometry. After harvesting, cells were distributed into a 96-well plate (1 x 10^6 cells per condition in duplicate). The cell surface F_c receptors were blocked by adding 100 µl of 10% (v/v) heat-inactivated human serum in PBS to each well for 1 minute. The blocking solution was pipetted out of the wells after centrifugation at 500 x *g* for 5 minutes. The cells were resuspended in 100 µl of 1.5% (w/v) paraformaldehyde in PBS and incubated for 30 minutes to fix the cells. Fixing the cells is essential for maintaining cell structure and shape (Covarrubias et al., 2019). A 5X diluted antibody mix was made by diluting 1 part antibody in 5 parts 1% (w/v) bovine serum albumin in PBS (BSA/PBS) and then added to the cells and incubated for 30 minutes. The antibodies used included allophycocyanin (APC) -conjugated monoclonal anti-human CD80 Antibody (BioLegend, San Diego, California) and fluorescein isothiocyanate (FITC)-conjugated monoclonal anti-human CD206 (MMR) antibody (BioLegend, San Diego, California) with wavelength excitation and emission at 675/25 nm and 533/30 nm, respectively. Finally, stained cells were washed twice in 100 µl 0.1% (v/v) Triton X in PBS at 800 x *g* for 8 minutes and resuspended in 1% (w/v) BSA in PBS. The median fluorescence intensity (MFI) of 50,000 cells was captured alongside that of unstained cells serving as the auto-fluorescence control on a BD Accuri C6 flow cytometer (BD Biosciences, Franklin Lakes, New Jersey). The

experiment was repeated on three biological replicates with two technical repeats for each experiment.

2.8 Gene expression

2.8.1 RNA extraction

To quantify the expression of inflammatory mediators, RNA was extracted from frozen M0, M1 and M2 macrophage cell pellets (1 x 10^6) using the Direct-zol RNA Miniprep kit (Zymo Research, Irvine, CA, USA). Each pellet was lysed in 700 µl of Trizol reagent followed by the addition of 700 µl of 100% (v/v) molecular grade EtOH (Sigma Aldrich St. Louis, Missouri). The solution was transferred into a Zymo-spin IICR column in a collection tube and centrifuged at 10 000 × *g* for 30 seconds at 4 °C. The centrifugation speed and temperature were maintained throughout the experiment. The resulting flow-through was discarded. DNase I treatment followed to remove any contaminating DNA. This involved the addition of 5 µl of DNase I and 75 µl of DNA digestion buffer complex directly to the column and incubating for 15 minutes at 25°C. RNA pre-wash (400 µl) was added to the column, the column was centrifuged, and the flow-through was discarded. The RNA-prewash was performed twice followed by an RNA wash with 700 µl of the RNA wash buffer, and centrifugation this time for 2 minutes. To elute the isolated RNA, the column was transferred into a 2 ml microcentrifuge tube and 30 µl of nuclease-free water (BioConcept, Allschwil, Switzerland) was added and centrifuged for 1 minute. The extracted RNA was stored at -80°C.

2.8.2 RNA purity and integrity

To confirm the quality of the extracted RNA, RNA purity was determined by an A260/A280 ratio of approximately 2.0 as well as an A230/A260 ratio in the range of 2.0 – 2.2, as determined using a Nanodrop One Spectrophotometer (Thermo Fisher Scientific, Waltham, Massachusetts). The RNA integrity of each sample was confirmed by gel electrophoresis with 1% (w/v) agarose in 1X tris-borate-EDTA (TBE) buffer. The TBE buffer was made with 2 mM ethylenediaminetetraacetic (EDTA), distilled water, 89 mM of Trizma base and boric acid (Sigma Aldrich St. Louis, Missouri). To enable visualisation of RNA bands after electrophoresis, 0.6 µg/ml ethidium bromide (Sigma Aldrich St. Louis, Missouri) was added to the agarose gel. 500 ng of total RNA extracted from each sample was loaded on the gel and subsequently loaded for electrophoresis at 100V for 1 h. Upon completion of electrophoresis, gels were viewed on the Gel Doc XR+ (BioRad, Hercules, California) to observe the bands representing the 28S and 18S rRNA that supports intact RNA.

2.8.3 cDNA synthesis

To obtain cDNA, the RevertAid First Strand cDNA Synthesis Kit (Thermo Fisher Scientific, Waltham, Massachusetts) was used to convert 250 ng of intact and pure RNA obtained from each sample into complementary DNA (cDNA). The manufacturer's protocol was followed to prepare the cDNA reaction (Table 2.1). cDNA synthesis was completed following a 60-minute incubation period at 42 °C, and subsequent incubation at 70 °C for 5 minutes to terminate the reaction. cDNA obtained was used immediately for quantitative PCR (qPCR).

Table 2.1: **cDNA synthesis reaction preparation**

Component	**Volume (µl)**
Template RNA	The volume that gives 250 ng
Oligo (dT) Primer	1
Nuclease Free Water	Up To 12
5x Reaction Buffer	4
RiboLock RNase Inhibitor	1
10 mM dNTP Mix	2
RevertAid RT	1
Final Volume	20

2.8.4 Quantitative PCR (qPCR)

Quantitative PCR was used to measure the gene expression of the inflammatory mediators *RIG-I, IL-1β, CXCL-10, CCL-2* and *IL-10* (Table 2.2). Primers for all the genes considered were designed using Primer3 (https://primer3.ut.ee/) except for the tyrosine 3 monooxygenase/tryptophan 5-monooxygenase activation protein zeta (*YWHAZ)* and ubiquitin C (*UBC)* primer sequences, which were obtained from Vandesompele et al. (2002). Each treatment condition was assessed in three biological replicates with two technical replicates for each sample. *YWHAZ* and *UBC* were selected as housekeeping genes for their stable expression in macrophages (Vandesompele et al., 2002; Oturai et al., 2016). Tris-EDTA buffer was used to reconstitute lyophilised primers (IDT Coralville, Iowa) into 100 µM stocks, which were diluted down into 10 µM working stock with nuclease-free water. To prevent freeze-thaw cycles, aliquots were made and stored at -20 °C. Primer efficiencies were determined with a serial dilution of cDNA for each gene of interest. A standard curve was plotted with the average

C_T values against the log of the cDNA concentration. Using the slope, the primer efficiency was determined using the formula below:

$$\text{Efficiency (\%)} = \left(10^{-\frac{1}{slope}} - 1\right) X\ 100$$

For all the genes of interest, the efficiency ranged between 95% and 105%. A Luna Universal qPCR Master Mix (NEB Ipswich, Massachusetts) was used to prepare the qPCR reactions containing primers for each of the genes considered (Table 2.3). Amplification (Table 2.4) and melt curve analysis followed using a CFX96 Touch Real-Time Detection System (Bio-Rad, Hercules, California). After a complete qPCR run, the baseline threshold was adjusted to 50 for all runs while obtaining the cycle threshold (C_T) values. The normalised expression was determined with the $\Delta\ C_T$ method using two reference genes by means of the following equation:

$$\text{Normalized Expression} = \frac{Relative\ quantity\ of\ Gene\ of\ Interest}{Relative\ quantity\ (YWHAZ)\ X\ Relative\ quantity\ (UBC)}$$

Where,

$$\text{Relative quantity} = \text{Efficiency of primer}^{\ (C_{qmin} - C_{qmax})}$$

The normalised expression values were subjected to further statistical analysis.

Table 2.2: Primer sequences used for gene expression analysis

Gene	Protein Encoded	Primer sequence (5 '- 3 ')
UBC	Ubiquitin C	**F**: ATTTGGGTCGCGGTTCTTG **R**: TGCCTTGACATTCTCGATGT
YWHAZ	Tyrosine 3-Monooxygenase/Tryptophan 5-Monooxygenase Activation Protein, Zeta	**F**: ACTTTTGGTACATTGTGGCTTCA **R**: CCGCCAGGACAAACCAGTAT
RIG-I	Retinoic acid-Inducible Gene I	**F**: TGTGCTCCTACAGGTTGTGGA **R**: CACTGGGATCTGATTCGCAAAA
IL-1β	Interleukin-1 beta	**F**: TCGCCAGTGAAATGATGGCT **R**: GGTCGGAGATTCGTAGCTGG
CXCL-10	C-X-C Motif Chemokine Ligand 10	**F**: TCTAAGTGGCATTCAAGG AGT **R**: TCAGACATCTCTTCTCACCC
CCL-2	C-C Motif Chemokine Ligand 2	**F**: CCCAAAGAAGCTGTGATCTTCA **R**: TGTGGAGTGAGTGTTCAAGT
IL-10	Interleukin-10	**F**: GCCTAACATGCTTCGAGAT **R**: GCAACCCAGGTAACCCTTA

Table 2.3: qPCR master mix preparation

Component	Gene	Volume (µl)	Final concentration
Luna Universal qPCR Master Mix		5	1x
Forward primer	*RIG-I, YWHAZ, CCL-2, TNF-α*	0.25	250 nM
	IL-1β	0.2	200 nM
	IL-10	0.4	400 nM
	CXCL-10	0.15	150 nM
	UBC	0.12	120 nM
Reverse primer	*RIG-I, YWHAZ, CCL-2, TNF-α*	0.25	250 nM
	IL-1β	0.2	200 nM
	IL-10	0.4	400 nM
	CXCL-10	0.15	150 nM
	UBC	0.12	120 nM
Template DNA		0.5	
Nuclease-free water		To 10	

Table 2.4: Thermal cycling conditions for gene expression analysis

Cycle step	Temperature (°C)	Time (Seconds)	Cycles
Initial Denaturation	95	60	1
Denaturation	95	15	40
Annealing and extension	60	30	
Melt Curve	60 – 95	5	1

2.9 Treatment conditions and transfection

To mimic a viral response, M0, M1, and M2 macrophages were transfected with 5’ triphosphate double-stranded RNA (5'ppp-dsRNA), a RIG-I agonist, for 2 hours. Each phenotype had three treatment conditions comprising of the untreated control, the 5'ppp-dsRNA transfected cells and the negative transfection control. RIG-I signalling was induced through transfection with 1 µg/ml 5'ppp-dsRNA (InvivoGen San Diego, California). To achieve transfection, 5'ppp-

dsRNA was added to 100 µl of Lyovec (InvivoGen San Diego, California), a lyophilised lipid-based transfection reagent, to form a transfection complex. The complex was incubated at 25 °C for 1 h before being added to the cells. To account for the effects of transfection, a negative transfection control was included where 100 µl of lyovec without 5'ppp-dsRNA was added. Changes in gene expression were determined as described in section 2.8.

2.10 Data analysis

IBM SPSS Statistics 29.0.2.0 (20) software was used to perform all statistical analyses. Technical repeat outliers from flow cytometry and RT-qPCR data were removed before analysis. To assess the differences in surface marker expression and inflammatory mediator expression between M0, M1 and M2 macrophages and in response to RIG-1 stimulation, one-way Analysis of Variance (ANOVA) was performed with Fisher's LSD post hoc comparisons ($n = 3$). To meet the assumption of a one-way ANOVA, Levene's test for equality of variance was also evaluated. A p-value of < 0.050 was considered significant.

CHAPTER 3: RESULTS

3.1 THP-1 cells differentiated in the presence of 1,25D$_3$ exhibited macrophage-like morphology

To confirm differentiation, microscopy was used to visualise THP-1 cells (Fig. 3.1A) differentiated with 5 nM PMA in the absence (Fig. 3.1B) and presence (Fig. 3.1C) of 10 nM 1,25D$_3$ for 96 hours. Regardless of the differentiation protocol, macrophages exhibited strong cell adherence and flattening, and increased size relative to the slightly oval-shaped and smooth-surfaced undifferentiated THP-1 cells. In the absence of 1,25D$_3$, differentiated macrophages showed an increase in size and irregularity in shape. However, the presence of 1,25D$_3$ caused macrophages to appear larger and adopt an amoebic shape with elongated spindle-like projections, which are morphological characteristics associated with primary macrophages as seen in Fig. 3.1D (TMS, 2019). Notably, differentiation significantly (Fig 3.2: $p < 0.050$) impacted cell viability regardless of the protocol used. Nonetheless, macrophage viability remained above 90% in both cases.

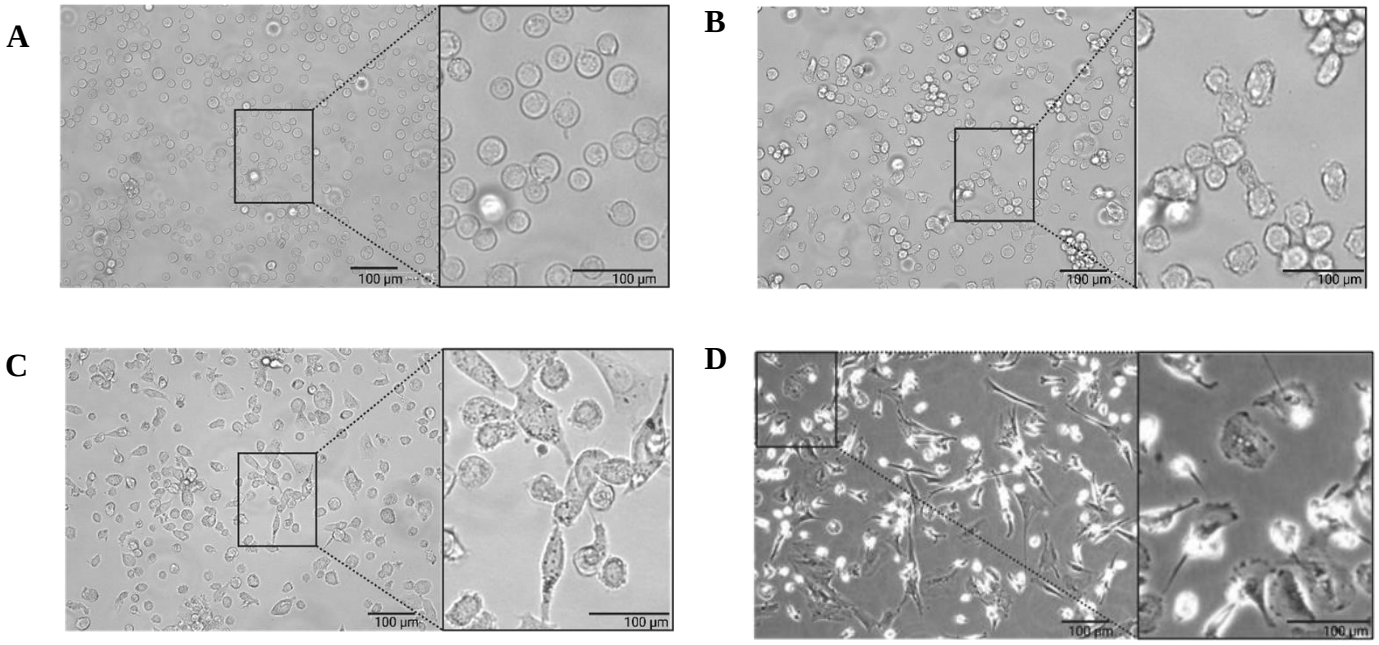

Figure 3.1: THP-1 macrophage differentiation was enhanced with 1,25D$_3$. Micrographs showing the morphological characteristics of THP-I monocytes (A) and alterations following differentiation. The differentiation entails the use of 5 nM phorbol 12-myristate 13-acetate (PMA) in the absence (B) and presence (C) of 10 nM 1,25D$_3$ for 96 h to obtain mature macrophages, which were compared to primary macrophages (D; primary macrophage image taken from TMS-lab.com).

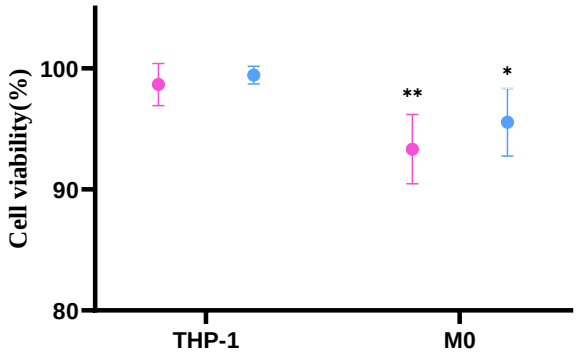

Figure 3.2: Differentiation of THP-1 cells reduced cell viability.
An error bar plot showing the percentage cell viability of undifferentiated THP-I cells compared to M0 macrophages obtained from the differentiation of THP-I cells with 5 nM PMA in the absence (pink) and presence (blue) of 10 nM $1,25D_3$. A one-way ANOVA confirmed the overall variance in viability between undifferentiated and differentiated cells, with pairwise LSD comparisons shown relative to the undifferentiated cells (*$p < 0.050$, ** $p < 0.010$). Error bars show the 95% CI (n = 3).

3.2 The presence of $1,25D_3$ during differentiation supports polarisation into both M1 and M2 phenotypes

To assess the effect of $1,25D_3$ during differentiation on macrophage polarisation, a flow cytometric analysis was employed. Exposure of naïve macrophages to IFN-γ and LPS resulted in a significant increase in CD80 levels compared to the control and cells treated with IL4 and IL13, regardless of whether these macrophages were derived from THP-1 in the presence or absence of $1,25D_3$ (Fig. 3.3A and B; $p < 0.010$). In fact, there was no significant difference in CD80 levels between macrophages derived from THP-1 differentiated in the presence or absence of $1,25D_3$ upon treatment with IFN-γ and LPS. However, macrophages derived from THP-1 in the absence, but not in the presence, of $1,25D_3$ also showed a significant increase in CD206 expression upon treatment with IFN-γ and LPS (Fig.3.3C; $p < 0.050$). Similarly, exposure of naïve macrophages to IL-4 and IL-13 resulted in a significant increase in CD206 levels compared to the control, regardless of whether these macrophages were derived from THP-1 in the presence ($p < 0.050$) or absence ($p < 0.010$) of $1,25D_3$ (Fig. 3.3C and D). Again, no significant difference was observed in CD206 levels between macrophages derived from THP-1 in the presence or absence of $1,25D_3$ upon treatment with IL-4 and IL-13. However, the CD206 levels in macrophages derived from THP-1 in the presence, but not in the absence, of $1,25D_3$ was significantly higher in cells treated with IL-4 and IL-13 compared to those treated with IFN-γ and LPS (Fig. 3.3D; $p < 0.050$). Notably, cell viability was not significantly

impacted in response to treatments, regardless of whether cells were differentiated in the presence or absence of 1,25D_3 (Fig. 3.4)

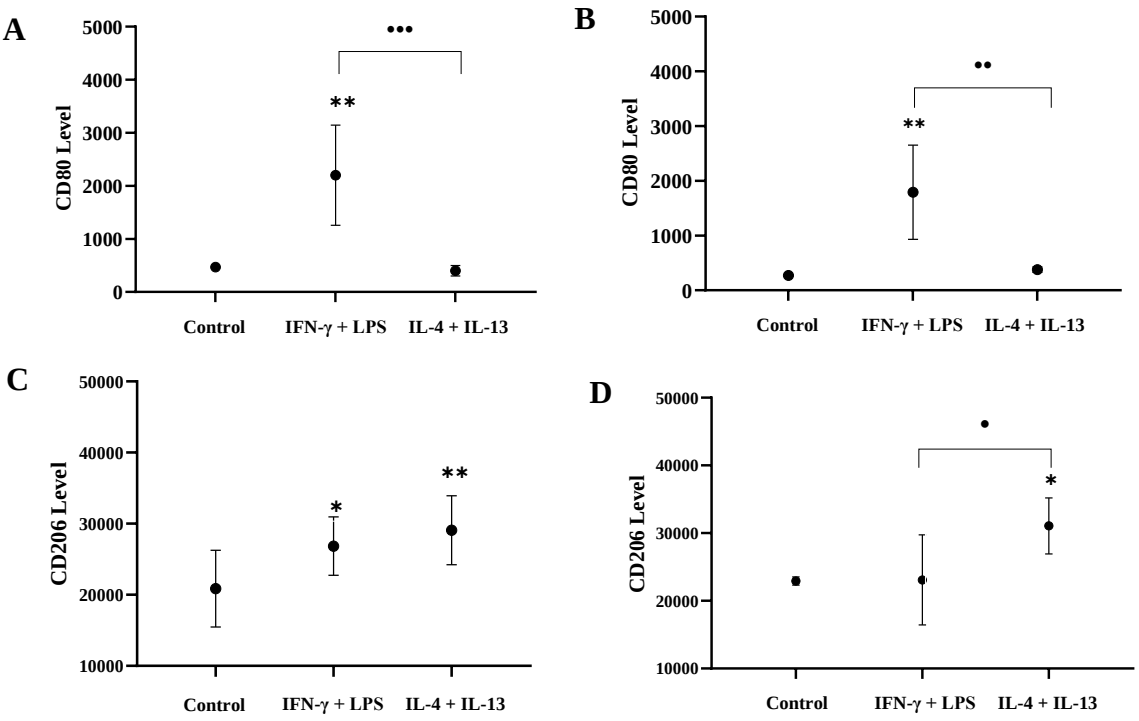

Figure 3.3: The presence of 1,25D_3 during differentiation supports distinct polarisation states. Error bar plot showing the changes in the expression of M1 (CD80) and M2 (CD206) polarisation markers in THP-1-derived naïve macrophages (control) obtained through treatment of THP-1 cells with 5 nM PMA in the absence (A and C) presence (B and D) of 10 nM 1,25D_3 following exposure to either 20 ng/ml IFN-γ and 100 ng/ml LPS (M1-inducing agents) or 20 ng/ml IL-4 and IL-13 (M2-inducing agents). A one-way ANOVA was used to determine significant differences, followed by an LSD post-hoc test. Pairwise comparisons are shown relative to the control (*$p < 0.050$, ** $p < 0.010$, *** $p < 0.001$) and between treatments (• $p < 0.050$, •• $p < 0.010$, ••• $p < 0.001$). Error bars show the 95% CI (n = 3).

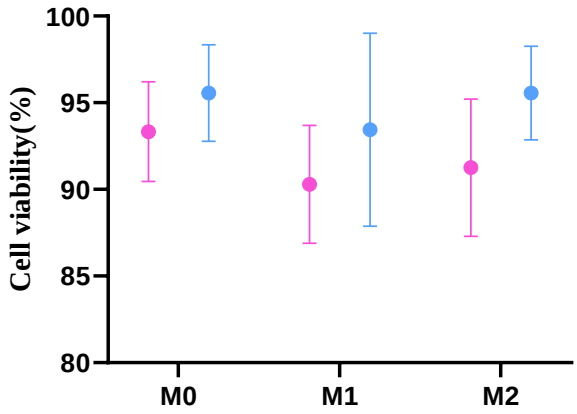

Figure 3.4: Polarisation into M1 and M2 macrophages did not impact cell viability. Error bar plots showing the percentage cell viability of M1 and M2 macrophages derived from THP-1 differentiated with 5 nM PMA in the absence (pink) and presence (blue) of 10 nM $1,25D_3$. Error bars show the 95% CI (n = 3).

3.3 Gene expression

3.3.1 Quality control

To confirm that the isolated RNA was pure and free from contamination (including phenols), the A260/280 and A260/230 ratios were determined. The A260/280 and A260/230 ratios ranged between 1.8 - 2.0 and 2.0 - 2.2, respectively. Gel electrophoresis was also employed to assess the integrity of the isolated RNA, which was indicated by the appearance of the 28S and 18S rRNA subunits, as two distinct bands on the gel (Fig. 3.5). However, the 2:1 band intensity ratio of 28S and 18S was not observed (Appendix 1). A 3% agarose gel electrophoresis was employed to confirm that amplicons of the expected size were amplified during RT-qPCR for all the gene transcripts considered (Fig. 3.6). Single PCR products (Fig. 3.6 and 3.7) were obtained for all genes with, sizes matching that predicted using *in silico* PCR (https://genome.ucsc.edu/cgi-bin/hgPcr). Furthermore, no products were amplified in the no-template controls (NTCs).

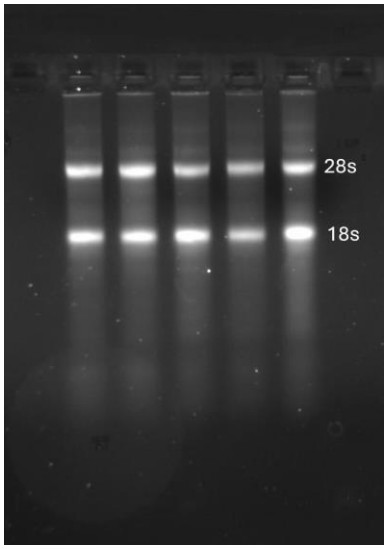

Figure 3.5: A representative image of an agarose gel for extracted RNA. An agarose gel showcasing two distinct bands representing the 28s and 18s rRNA subunits, indicating the integrity of the RNA extracted.

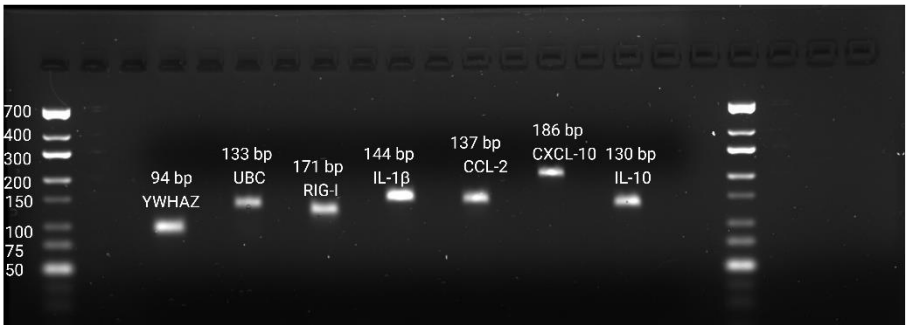

Figure 3.6: A representative agarose gel showing the RT-qPCR products following amplification. Image of representative 3% agarose gel displaying the RT-qPCR products obtained following amplification of reference genes (*YWHAZ and UBC*) and target genes considered (*RIG-I, IL-1β, CCL-2, CXCL-10 and IL-10*). Each product had a single band with base pair sizes corresponding to the expected sizes, as measured with a TriDye Ultra-low range DNA ladder (New England Biolabs, Ipswich, Massachusetts).

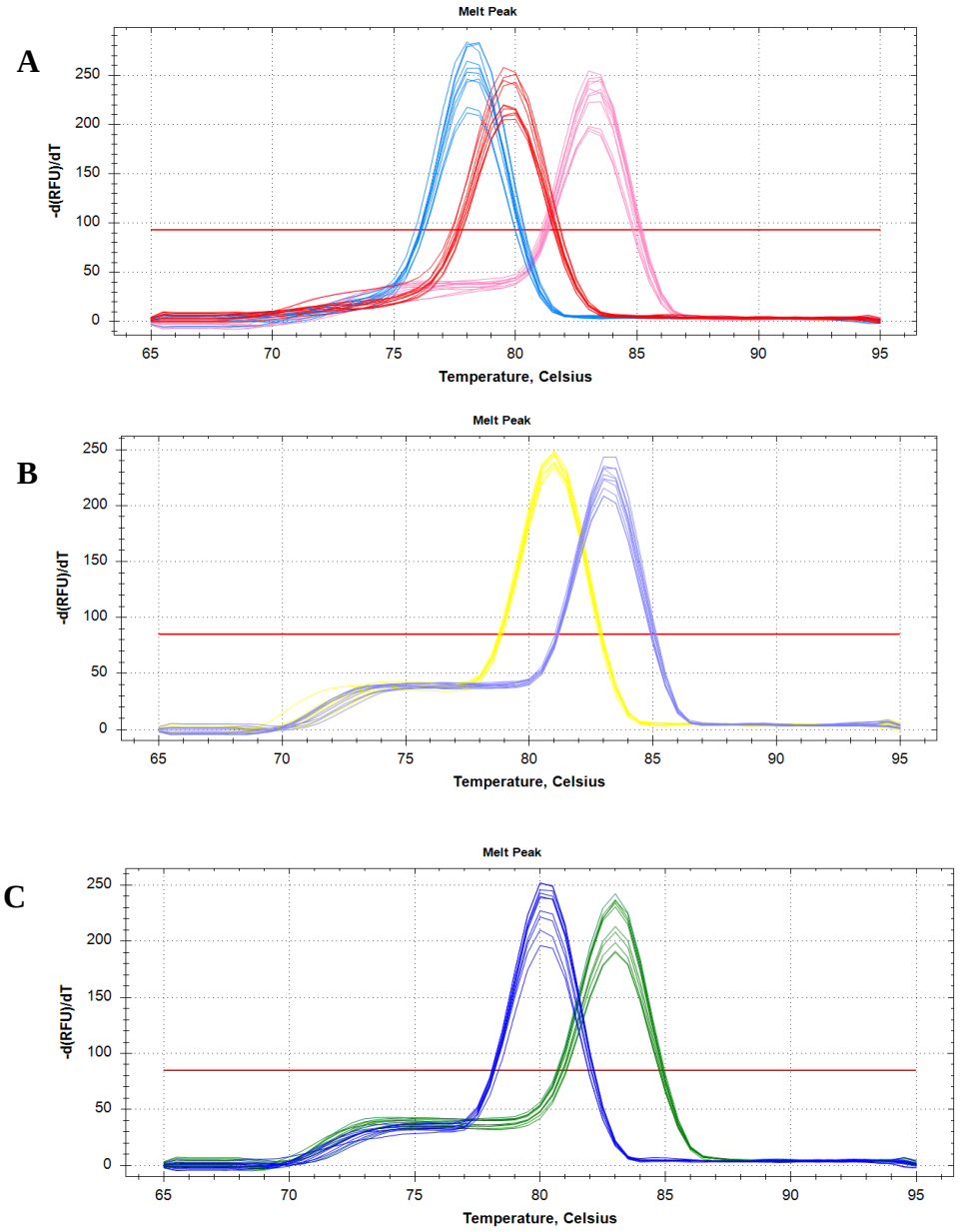

Figure 3.7: Representative melt curves from amplification of candidate genes. Screen capture images of melt curves obtained from the Bio-Rad CFX Maestro 1.0 software showing the relative change in fluorescence with time (-d(RFU)/dT) against temperature in Celsius (°C). The images show the melt peaks of the genes considered including *RIG-I* (A; blue), *IL-Iβ* (A; pink), *CCL-2* (B; Purple), *IL-10* (B; Yellow), *CXCL-10* (C; Dark blue) and the reference genes *YWHAZ* (A; Red) and *UBC* (C; Green).

3.3.2 M1 macrophages express higher levels of pro-inflammatory mediators

To quantify changes in the expression of inflammatory mediators, the baseline expression levels of *RIG-1*, *IL-1β*, *CCL-2*, *CXCL-10* and *IL-10* were quantified in M0, M1 and M2 macrophages differentiated in the presence and absence of 10 nM $1,25D_3$ (Fig. 3.8). M1 macrophages showed significantly higher mRNA levels of *RIG-I* ($p < 0.010$ and $p < 0.001$, Fig. 3.8A), *IL-1β* ($p < 0.010$ and $p < 0.001$; Fig. 3.8B), *CCL-2* ($p < 0.001$; Fig. 3.8C), and *CXCL-10* ($p < 0.010$ and $p < 0.001$; Fig. 3.8D) compared to M0 macrophages, both in the absence and presence of $1,25D_3$. Similarly, regardless of $1,25D_3$ presence, M2 macrophages showed significantly higher mRNA levels of *IL-10* compared to M0 macrophages ($p < 0.001$ Fig. 3.8E). Interestingly, *RIG-I* ($p < 0.010$) and *CXCL-10* ($p < 0.050$) expression were significantly higher in M1 macrophages differentiated in the presence of $1,25D_3$ compared to those differentiated in the absence of $1,25D_3$.

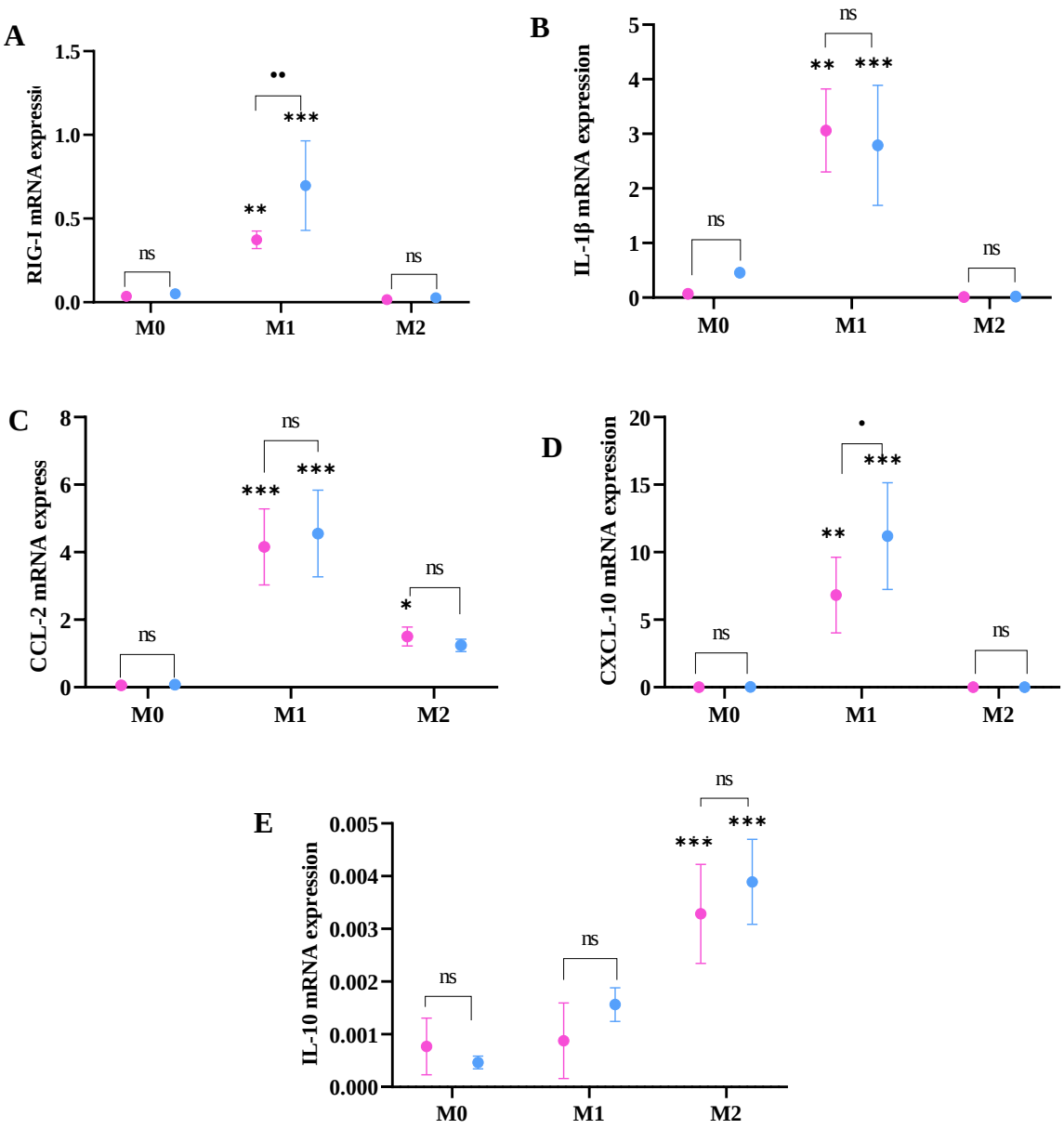

Figure 3.8: Baseline expression of inflammatory markers in M0, M1 and M2 macrophages. Error bar plot showing the baseline expression of inflammatory markers (*RIG-1*, *IL-1β*, *CCL-2*, *CXCL-10*) and anti-inflammatory *IL-10* in M0, M1 and M2 macrophages differentiated in the presence (blue) and absence (pink) of $1,25D_3$. Significance was determined by a one-way ANOVA with LSD pairwise comparisons made relative to M0 (* $p < 0.050$, ** $p < 0.010$, *** $p < 0.001$) and between polarisation states in the absence and presence of $1,25D_3$ (• $p < 0.010$, •• $p < 0.010$, ••• $p < 0.001$). Error bars show the 95% CI (n = 3).

3.4. Transfection treatment outcomes

To assess the functional impact of the differentiation of THP-1 into macrophages in the absence and presence of $1,25D_3$, a viral response was simulated in M0, M1 and M2 macrophages. This was achieved by transfection with 5'ppp-dsRNA, a RIG-I agonist.

3.4.1 Transfection quality control

3.4.1.1 The negative transfection control and untreated cells had comparable expression levels of target genes

To confirm that the transfection procedure itself did not alter gene expression, gene expression was compared between the negative transfection control (uncomplexed lyovec solution) and the respective untransfected cells. Regardless of the differentiation protocol applied, no significant difference in gene expression was observed between the untransfected cells and the negative transfection control in either M0, M1 or M2 macrophages (Fig. 3.9).

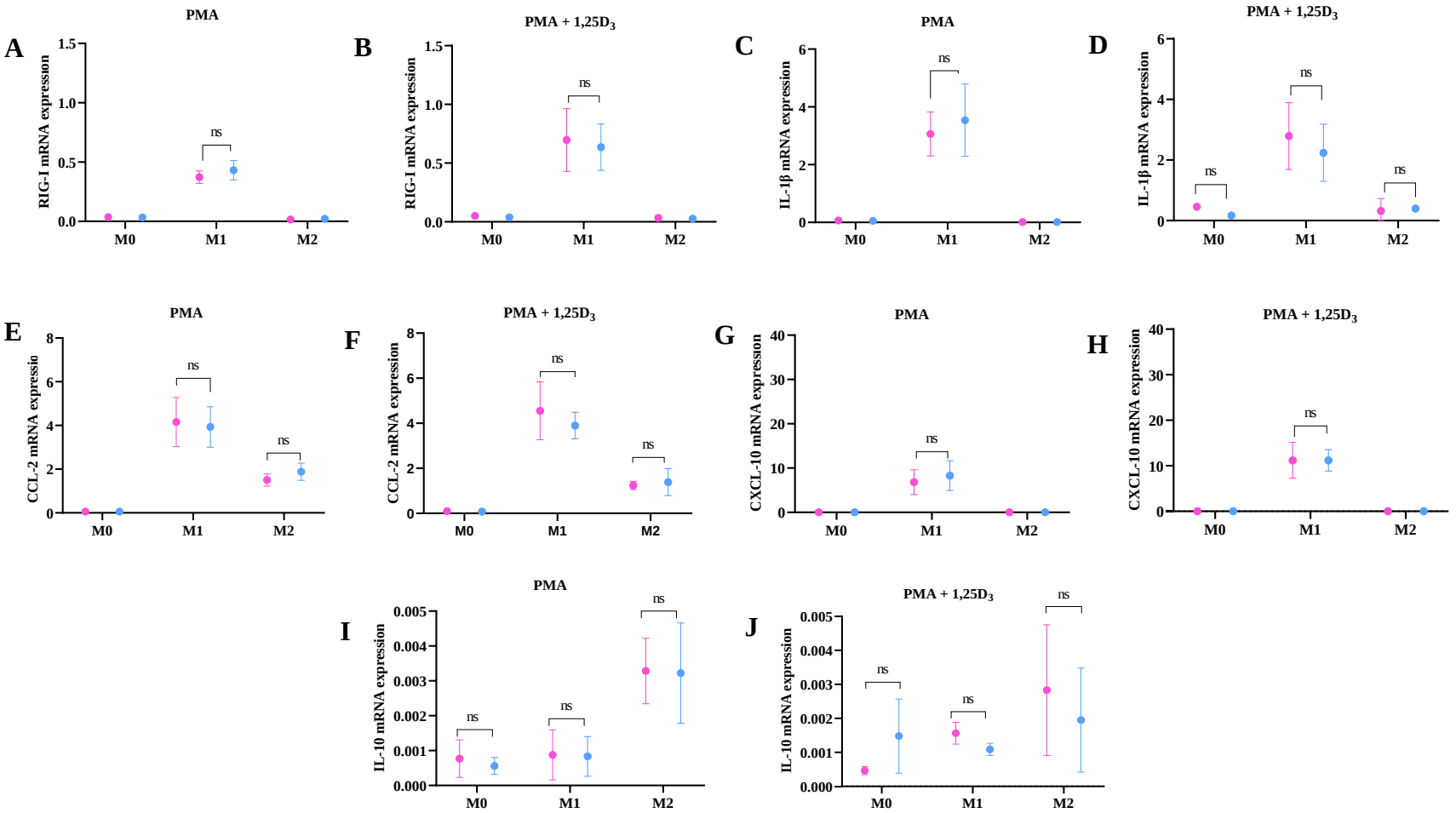

Figure 3.9: Transfection did not impact the experimental outcome. Error bar plot showing the expression levels of *RIG-I* (A and B), *IL-Iβ* (C and D), *CCL-2* (E and F), *CXCL-10* (G and H), and *IL-10* (I and J) in the untreated (pink) control and negative transfection control (blue) for M0, M1, and M2 macrophages differentiated in the absence (A, C, E, G, I) and presence (B, D, F, H, J) of 10 nM $1,25D_3$. Significance was determined by a one-way ANOVA with LSD pairwise comparisons made within each phenotype in the absence and presence of $1,25D_3$ (• $p < 0.010$, •• $p < 0.010$, ••• $p < 0.001$). Error bars show the 95% CI (n = 3).

3.4.1.2 Cell viability was maintained post-transfection

To confirm that the transfection procedure did not impact cell viability, cell viability was assessed 2 hours post-transfection to match the time chosen for the transfection. The cell viability was determined in the untreated control, as well as 5' ppp-dsRNA-transfected M0 (Fig. 3.10A), M1(Fig. 3.10B) and M2 (Fig. 3.10C) macrophages differentiated in the absence and presence of 1,25D_3. No significant difference in cell viability was observed between the untransfected controls and 5'ppp-dsRNA-transfected cells for M0, M1, or M2 macrophages, regardless of differentiation protocol.

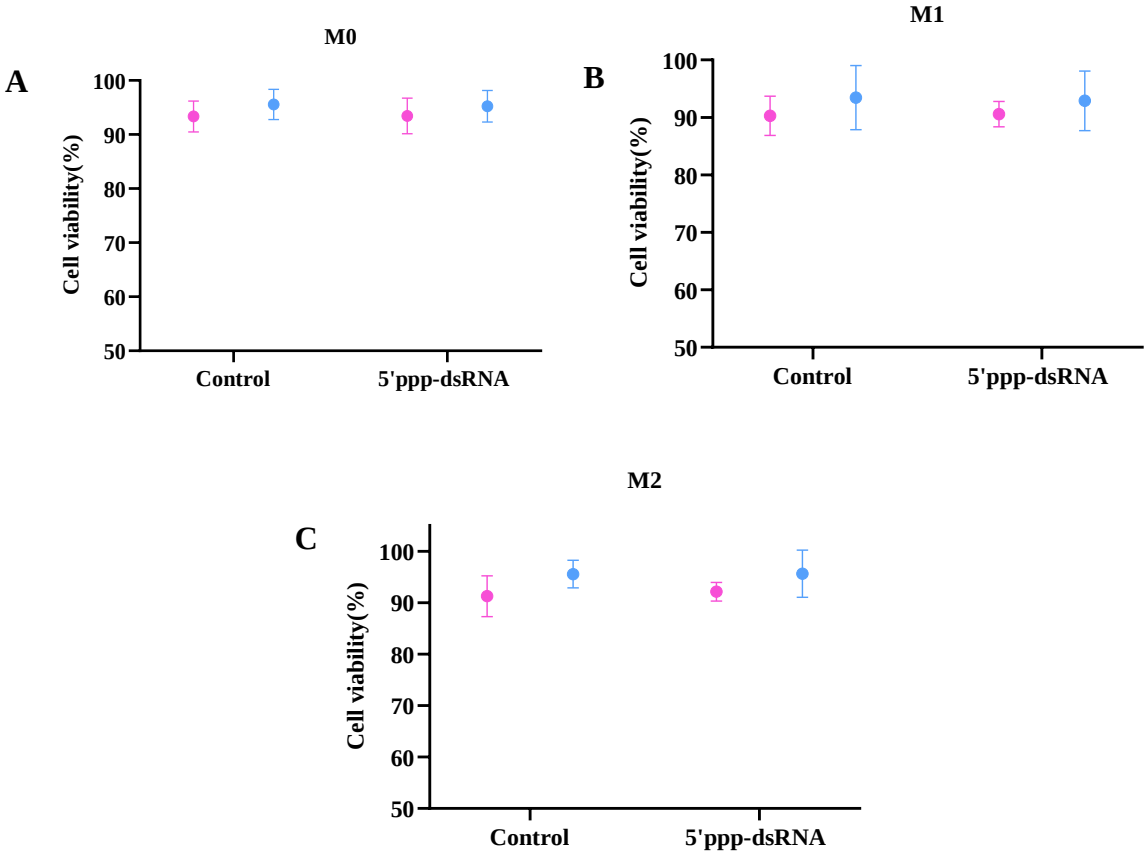

Figure 3.10: Transfection did not impact cell viability. Error bar plots showing the percentage of viable cells in the untreated controls (pink) compared to 5'ppp-dsRNA-treated cells (blue) in M0 (A), M1 (B) and M2 (C) macrophages differentiated in the absence and presence of 10 nM 1,25D_3. A one-way ANOVA was used to determine significant differences, followed by an LSD post-hoc test. Pairwise comparisons were determined relative to the control and between the absence and presence of 1,25D_3 in the untreated control and 5'ppp-dsRNA treated cells (•• $p < 0.010$, ••• $p < 0.001$). Error bars show the 95% CI (n = 3).

3.4.2 RIG-I stimulation caused varied expression of target genes in M0, M1 and M2 macrophages.

After transfection with 5'ppp-dsRNA for 2 hours, macrophages were assessed for changes in the expression levels of target genes. These changes were determined relative to the control and between cells differentiated in the presence and absence of $1,25D_3$. M0 (Fig. 3.11A) and M1 (Fig. 3.11B) macrophages did not experience a significant change in gene expression following transfection with 5'ppp-dsRNA, regardless of the absence or presence of $1,25D_3$. In contrast, transfection with 5'ppp-dsRNA significantly increased *CXCL-10* (Fig. 3.11C), expression in M2 macrophages differentiated in the presence of $1,25D_3$ relative to the control ($p < 0.001$) and compared to cells differentiated in the absence of $1,25D_3$ ($p < 0.001$). There was a significant difference in *IL-Iβ* expression in M2 macrophages differentiated in the presence of 1,25D relative to cells differentiated with only PMA (Fig. 3.11C; $p < 0.050$). However, regardless of the varying expression levels in the presence and absence of $1,25D_3$, there was no significant difference relative to the control. Similarly, *CCL-2* expression in M2 macrophages was significant in the presence of $1,25D_3$ relative to the control (Fig. 3.11C; $p < 0.050$). Interestingly, the expression levels of *RIG-I* and *IL-10* 2 hours post-transfection were comparable to the controls and not significant in the presence or absence of $1,25D_3$.

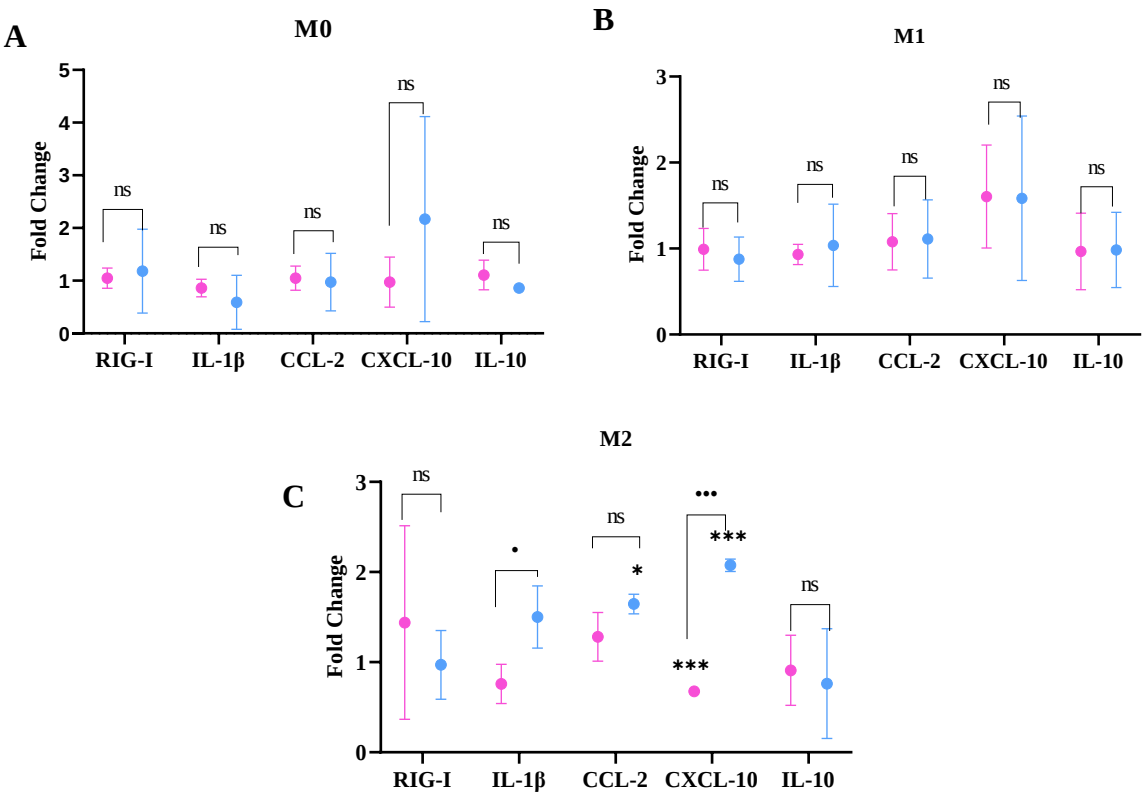

Figure 3.11: **Expression of *CCL-2* and *CXCL-10* were elevated in M2 macrophages 2 hours post-transfection with 5'ppp-dsRNA**. Fold change of inflammatory mediators 2 h post-transfection with 5'ppp-dsRNA in M0(A) M1 (B) and M2 (C) polarised macrophages obtained from THP-1 cells differentiated without (pink) and with (blue) 1,25D_3. Differences between the control (at 1) and 5'ppp-dsRNA transfected cells for each gene are shown (* $p < 0.050$, ** $p < 0.010$, *** $p < 0.001$) and between groups with and without 1,25D_3. (• $p < 0.010$, ••• $p < 0.001$). Error bars show the 95% CI (n = 3).

CHAPTER 4: DISCUSSION

The THP-1 promonocytic cell line has long been a preferred model for the study of macrophage biology. However, the lack of uniformity in the protocols used over time to obtain naive macrophages has contributed to inconsistencies in research outcomes. For example, the use of high concentrations of PMA induces the expression of elevated levels of inflammatory markers and other genes after differentiation, interfering with experimental outcomes after further stimulation (Maeß et al., 2014; Lund et al., 2016). Additionally, this PMA-induced inflammatory state has been reported to impair polarisation of cells into the M2 state (Maeß et al., 2014). Results from this study confirmed low-dose PMA as sufficient to cause monocyte-macrophage differentiation without activating an inflammatory state before added stimulation. Furthermore, $1,25D_3$, as an addition to the low-dose PMA differentiation protocol, resulted in a more macrophage-like phenotype that maintained an inactivated state at baseline prior to treatments (Mol et al., 2024). Additionally, macrophages obtained in the presence of $1,25D_3$ were polarised successfully into distinct M1 and M2 phenotypes, expressing significantly more of only the M1 marker upon IFN-γ and LPS treatment and only the M2 marker upon IL-4 and IL-13 treatment relative to the control. Finally, the low-dose PMA and $1,25D_3$ protocol supported the functional capability of the M2 polarised state.

Prior to gene expression analysis, the RNA quality had to be assessed. Notably, the intensity of the 18S band was generally slightly higher than that of the 28S band. While the 2:1 ratio of 28S:18S has been widely used as an indication of RNA integrity, according to Imbeaud et al. (2005) this indicator is inconsistent and subjective. This is because the appearance is impacted by various conditions such as the amount of RNA used, the electrophoresis set up and the fluorescence intensity of the ethidium bromide utilised. A better means of assessing RNA quality would be to determine individual RIN numbers using a bioanalyser. Given that both 28S and 18S bands were clearly visible in this study, RNA quality was deemed acceptable for further analysis.

Regardless of the differentiation protocol applied (with vs without $1,25D_3$) in this study, cell viability remained high, with an average cell viability of 94% and 95.3% recorded after differentiation with 5 nM PMA in the absence or presence of 10 nM $1,25D_3$, respectively. The high viability recorded suggests that a lower PMA concentration may result in less cytotoxicity. This is consistent with a handful of studies that have reported improved cell survival upon utilising relatively low PMA concentrations to obtain macrophages with or without resting

periods. For instance, (Biriken, 2019) recorded a 92.2% cell viability following differentiation with 20 ng/ml of PMA. Lund et al. (2016) reported a 93% viability post-stimulation with 5 ng/ml of PMA after 48 h. Similarly, Browne et al. (2022) also reported 92.5% cell viability following 72 h of exposure with 15 ng/ml PMA. This was, however, not the case where higher concentrations of PMA were used, as seen by a decline of cell viability to about 83.5% with 1000 ng/ml PMA stimulation (Browne et al., 2022). 5 nM is equivalent to 1.92 ng/ml. Across multiple studies, a high concentration of PMA was closely correlated to cases of apoptosis, as seen by the decrease in cell viability post-differentiation (Starr et al., 2018; T. Liu et al., 2023).

Notably, neither polarisation into the M1 or M2 phenotype significantly decreased cell viability, regardless of whether $1,25D_3$ was applied during cell differentiation. Following polarisation into M1 and M2 phenotypes, subsequent transfection for 2 h with 5' ppp-dsRNA did not cause any further decline in cell viability, despite the prolonged time in cell culture at this point. This was the case regardless of the protocol applied to obtain the macrophages (with vs without $1,25D_3$) and suggests a high transfection efficiency with successful agonist uptake by the cells (Neuhaus et al., 2016).

From a morphological point of view, cell adherence, flattening, size increase and irregularity in shape were observed in THP-1 cells differentiated in the presence of $1,25D_3$ compared to the cells differentiated with just PMA. Additionally, integrating $1,25D_3$ into the low-dose PMA protocol caused the macrophages obtained to attain a more primary macrophage-like morphology, characterised by a larger amoebic shape with large and elongated spindle projections, consistent with the classic features of macrophages as described by Lee et al. (2013) and Makaremi et al. (2019). The adherence, flattening and shape irregularity of differentiated macrophages are primarily attributed to the presence of PMA, which varies with the concentration used (Tsuchiya et al., 1980; Park et al., 2007; Daigneault et al., 2010). $1,25D_3$, which alone fails to give the expected morphological expression (Valdés López and Urcuqui-Inchima, 2018), proved to be a suitable complement to PMA to provide the required outcome of matured macrophages after differentiation. In agreement, Valdés López and Urcuqui-Inchima (2018) showed that the differentiation of the U937 monocytic cell line with PMA in addition to $1,25D_3$ caused the macrophages to acquire an ameboid morphology comparable to primary macrophages. Other factors such as the length of the resting period post-stimulation and the length of differentiation overall contribute to the outcome of differentiation (Daigneault et al., 2010; Pinto et al., 2021, 2020).

Regardless of the differentiation protocol, CD80, often described as a robust marker of the M1 phenotypic state, was significantly expressed in M1 macrophages obtained (Ambarus et al., 2012; Jaguin et al., 2013; Tarique et al., 2015). Similarly, the expression of CD206 was notable in M2 macrophages (Choi et al., 2010; Xu et al., 2020). These observations were consistent in the presence or absence of $1,25D_3$. A convenient conclusion would have been that $1,25D_3$ during differentiation did not matter or impact polarisation. Interestingly, however, M1 macrophages obtained from differentiation with just PMA also showed significant expression of CD206, an M2 macrophage marker. This is indicative of a form of overlap in the polarisation states. This is not uncommon and can be traced to the highly adaptable nature of macrophages. They exist on a continuum and, hence, are difficult to limit into a binary state, as the expression of phenotypic markers can change with time (Smith et al., 2016). Remarkably, the presence of $1,25D_3$ during differentiation resulted in an M1 macrophage with CD206 expression levels comparable to the untreated control. This suggests the capacity of $1,25D_3$ to cause polarisation into distinct states with less heterogeneity. This is particularly significant because high PMA concentrations have been linked to ineffective M2 polarisation (Maeß et al., 2014; He et al., 2021). It turns out that not only does the reduction in PMA concentration help with responsiveness to polarising stimuli, as suggested by Maeß et al. (2014), but also that augmentation with $1,25D_3$ ensures polarisation into distinct phenotypes. Significant expression of the inflammatory markers, *IL-Iβ, CXCL-10*, *CCL-2* and *RIG-I* in M1 macrophages (Sierra-Filardi et al., 2014; Liu et al., 2018; Tsai et al., 2019) and *IL-10* (Mantovani et al., 2002; Gordon and Martinez, 2010) in M2 macrophages, regardless of differentiation protocol, further confirms the polarisation states of the macrophages.

Introducing the M0, M1 and M2 macrophages obtained with the protocols employed to a viral challenge, provided a means to test their functional capacity in the first 2 h of infection. 5' ppp-dsRNA, a RIG-I agonist, was employed (Goulet et al., 2013; Chiang et al., 2015). After transfection with the RIG-I agonist, M0 macrophages showed no significant changes in the expression of the inflammatory markers evaluated in this study across the protocol considered. The undetected expression of the cytokine and any of the chemokines we evaluated could be a result of the short exposure time (Moradian et al., 2020; Thoresen et al., 2023). Similarly, the transfection of M1 macrophages with the RIG-I agonist did not increase their inflammatory state. This was consistent in cells differentiated in the presence or absence of $1,25D_3$. The lack of responsiveness of M1 macrophages to 5'ppp-dsRNA transfection, even after the expression of inflammatory markers at baseline, could also be a result of endotoxin tolerance. This is a

phenomenon where an earlier exposure to LPS causes a decline of pro-inflammatory cytokine expression following subsequent stimulation with other agents capable of causing inflammation. This occurs to prevent hyperinflammation and potential damage to the tissue (Cavaillon and Adib-Conquy, 2006; Rajaiah et al., 2013; Liu and Zhou, 2019). Alternatively, the changes in the inflammatory state may have at this point been more notable at the protein level.

There was no significant change in the expression of *RIG-I* in M2 macrophages, regardless of differentiation protocol in response to 5'ppp-dsRNA transfection. Interestingly, however, in M2 macrophages differentiated in the presence of $1,25D_3$, robust expression *of IL-1β, CCL-2*, and *CXCL-10* was observed in response to 5'ppp-dsRNA, which was not the case in the PMA-only differentiation protocol. The change in expression of *IL-1β, CCL-2*, and *CXCL-10* following stimulation by the RIG-I agonist, despite no observable changes in the expression of RIG-I itself can be explained by the study of Thoresen et al. (2023). Thoresen et al. (2023) found that a RIG-I response occurs in two phases. The first phase is led by the cytosolic resident pool of the RIG-I protein, which is capable of initiating a response upon recognition of a PAMP. This means that the pre-existing RIG-I in the cytoplasm can lead to an initial response without further expression. It is also possible that the two-hour treatment time in this study may have been too early to observe measurable changes in endogenous RIG-I expression.

A similar event was expected from M0 macrophages post-transfection, except that the delayed expression of inflammatory markers could be because the transition of M0 macrophages into a pro-inflammatory state happens relatively slower than an M2 - M1 phenotypic transition (Liu et al., 2020). M0 macrophages that are in a naïve state at baseline require priming and metabolic shifts, while M2 macrophages that have earlier assumed a functional state require less time to repolarise with the right environmental cues. The reprogramming of M2 macrophages into the M1 phenotype usually involves switching to glycolysis from oxidative phosphorylation (Van den Bossche et al., 2017). The concept of macrophage repolarisation is primarily dependent on the present microenvironment, with no memory of the previous state (Liu et al., 2020). The downregulation of the previously expressed *IL-10,* an anti-inflammatory marker, post-transfection is indicative of the initiation of an inflammatory response that is going on in the background. This is because the expression of marker genes associated with a macrophage state reflects the current state and not the state from which it was repolarised (Liu et al., 2020). The possible repolarisation of macrophages from M2 into the M1 state in this study occurred only in macrophages differentiated in the presence of $1,25D_3$. These results suggest that $1,25D_3$

supports macrophages in maintaining homoeostasis in the tissue. This was demonstrated by an improved M2 macrophage state, with the capacity to revert to an inflammatory phase in response to viral exposure. It is important to also note that these interventions were swift, as demonstrated by the reversion happening within 2 h post-transfection. A few hours more into our transfection time point, we may have had a look at how this phenomenon is likely to manifest in M0 and M1 macrophages. Possibly showing how the presence of $1,25D_3$ could support a robust expression of inflammatory cytokines to clear the viral infection transitioning M0 into M1 macrophages and increasing the prevalence of inflammatory cytokines in M1 macrophages to clear infection. The expression of proinflammatory markers in M2 macrophages treated with the RIG-I agonist is not an isolated case. In their study, Vogelpoel et al. (2014) reported the expression of proinflammatory cytokines such as IL-1β in M2 macrophages exposed to TLR agonists and complexed IgG. Similarly, Wu et al. (2023) also demonstrated that RIG-I activation reversed M2 macrophages caused by cigarette smoking into M1 macrophages.

Taken together, the PMA-only protocol was sufficient to maintain relatively high cell viability through differentiation, polarisation and transfection of the macrophages. While this may work, the result obtained from differentiation in the presence of $1,25D_3$ proves more effective in promoting even further a higher survival potential of cells as seen by the even higher cell viability. Similarly, to assume a more primary macrophage-comparable morphology, the addition of $1,25D_3$ was required. This extends to the distinct surface marker expression that minimises heterogeneity in the polarised macrophage population. Finally, while the exact action of $1,25D_3$ was not captured in M0 and M1 macrophages 2 hours post-transfection with 5' ppp-dsRNA, the swift repolarisation of M2 macrophages differentiated with $1,25D_3$ into M1 macrophages to facilitate pathogen clearance is indicative of the functional capacity of a $1,25D_3$-integrated low-PMA based differentiation protocol above that using just PMA.

CHAPTER 5: CONCLUSION

5.1 Summary of the results

The aim of this study was to evaluate the impact of $1,25D_3$ on low-dose PMA-based monocyte-to-macrophage differentiation, polarisation and functional potential. Taken together, the results show that the addition of 10 nM $1,25D_3$ to the differentiation protocol enhances differentiation and supports macrophage polarisation into distinct M1 and M2 phenotypes. Moreover, the presence of $1,25D_3$ enhanced the functional potential of M2 macrophages, with only M2 macrophages obtained from macrophages differentiated in the presence of $1,25D_3$ responding to an immune challenge. This result not only showcased the repolarisation ability of macrophages but also the impact of $1,25D_3$ in supporting a swift phenotypic change with changing environmental cues - in this case inflammation to clear out pathogens. Therefore, the findings from this study strongly support our hypothesis that the addition of $1,25D_3$ to a low-dose PMA-based differentiation protocol will yield mature, naive macrophages (M0) that can be polarised into a functional pro-inflammatory (M1) or anti-inflammatory (M2) phenotype.

5.2 Implication of Research Study

This research study supports deeper research into macrophage biology by providing a more suitable model for *in vitro* studies. At the same time, this study expands our knowledge of $1,25D_3$ function - stepping away from the classical anti-inflammatory role and into a broader immunomodulatory capacity. In this case, it appears to have the ability to prime macrophages for a better functional state, whether it is pro-inflammatory or anti-inflammatory. This ultimately suggests that the maintenance of a sufficient vitamin D status *in vivo,* is essential for supporting a healthy immune system, primed for defence.

5.3 Limitations of Study

In this research study, we only explored the expression of *RIG-I*, *IL-1β, CXCL-10, CCL-2* and *IL-10*, 2 h post-transfection with 5'ppp-dsRNA, a RIG-I agonist, at mRNA level. While these genes all play a functional role in macrophages and are inducible upon viral stimulus, the list is not exhaustive and there are many other candidate genes that could have been included to make the study more comprehensive. The choice of the 2 h time point targeting early responses may not have given a full picture of the expression of some of the key markers of immune cell signalling that may peak well after 2 h. Moreover, some changes may have only been apparent at the protein level. While THP-I cells exhibit more of the functional characteristics of primary macrophages compared to other monocytic cell lines such as U937 cells, many of the

differences remain between model cell lines and primary cells. It remains to be seen whether vitamin D supports similar roles in terms of macrophage polarisation and function in primary cells. Nonetheless the purpose of this study was specifically focused on *in vitro* cell models often used in immunological studies despite the difficulties in differentiating and polarising these cells.

5.4 Future Research Considerations

For a broader picture of the cytokine profile of polarised macrophages differentiated by the low-dose PMA and PMA+1,25D_3 protocol, 4, 6, 12 and/or 24 h timepoints should be considered. This is important to capture both early and late responses after stimulation. Furthermore, key inflammatory markers such as IFNα and β etc., should be evaluated for a holistic view of the cytokine profile of the macrophages obtained. Macrophage function transcends just intervention in viral infections. Hence, signalling pathways led by other PRRs such as the TLRs should be considered. Finally, the functional implications of these findings can be elucidated further by employing techniques such as RNA sequencing (RNA-seq) to provide a genome-wide comprehensive view of genes expressed by the macrophages obtained from the two protocols before and after stimulation of any kind.

REFERENCES

Adams, J.S., Hewison, M., 2008. Unexpected actions of vitamin D: New perspectives on the regulation of innate and adaptive immunity. Nat Clin Pract Endocrinol Metab. https://doi.org/10.1038/ncpendmet0716

Aldo, P.B., Craveiro, V., Guller, S., Mor, G., 2013. Effect of culture conditions on the phenotype of THP-1 monocyte cell line. American Journal of Reproductive Immunology 70, 80–86. https://doi.org/10.1111/aji.12129

Ambarus, C.A., Krausz, S., van Eijk, M., Hamann, J., Radstake, T.R.D.J., Reedquist, K.A., Tak, P.P., Baeten, D.L.P., 2012. Systematic validation of specific phenotypic markers for in vitro polarized human macrophages. J Immunol Methods 375, 196–206. https://doi.org/10.1016/j.jim.2011.10.013

Auffray, C., Sieweke, M.H., Geissmann, F., 2009. Blood monocytes: Development, heterogeneity, and relationship with dendritic cells. Annu Rev Immunol. https://doi.org/10.1146/annurev.immunol.021908.132557

Aziz, M.A., Krisnadi, S.R., Handono, B., Setiabudiawan, B., 2023. Pregnant Human Myometrial 1-41 Cell Viability Test on Vitamin D Administration. Althea Medical Journal 10. https://doi.org/10.15850/amj.v10n3.2750

Baxter, E.W., Graham, A.E., Re, N.A., Carr, I.M., Robinson, J.I., Mackie, S.L., Morgan, A.W., 2020. Standardized protocols for differentiation of THP-1 cells to macrophages with distinct M(IFNγ+LPS), M(IL-4) and M(IL-10) phenotypes. J Immunol Methods 478. https://doi.org/10.1016/j.jim.2019.112721

Bell, T.D., Demay, M.B., Burnett-Bowie, S.A.M., 2010. The Biology and Pathology of Vitamin D Control in Bone. J Cell Biochem 111, 7. https://doi.org/10.1002/JCB.22661

Biriken, D., 2019. Differentiation of Human Leukemia Monocyte Cells to Macrophage-Like Cells with Phorbol- 12-Myristate-13-Acetate. Journal of Ankara University Faculty of Medicine 72, 34–38. https://doi.org/10.4274/atfm.galenos.2019.02886

Browne, E., Kavanagh, S., Devery, S., 2022. The Cytotoxicity of Phorbol 12- Myristate 13-Acetate and Lipopolysaccharide on THP-1 Cells and an Optimized Differentiation Protocol. MDPI AG, p. 5. https://doi.org/10.3390/bitap-12785

Cannell, J.J., Vieth, R., Umhau, J.C., Holick, M.F., Grant, W.B., Madronich, S., Garland, C.F., Giovannucci, E., 2006. Epidemic influenza and vitamin D. Epidemiol Infect. https://doi.org/10.1017/S0950268806007175

Cavaillon, J.M., Adib-Conquy, M., 2006. Bench-to-bedside review: Endotoxin tolerance as a model of leukocyte reprogramming in sepsis. Crit Care. https://doi.org/10.1186/cc5055

Chadha, M.K., Fakih, M., Muindi, J., Tian, L., Mashtare, T., Johnson, C.S., Trump, D., 2011. Effect of 25-hydroxyvitamin D status on serological response to influenza vaccine in prostate cancer patients. Prostate 71, 368–372. https://doi.org/10.1002/pros.21250

Chanput, W., Mes, J.J., Wichers, H.J., 2014. THP-1 cell line: An in vitro cell model for immune modulation approach. Int Immunopharmacol. https://doi.org/10.1016/j.intimp.2014.08.002

Chen, Q., Ross, A.C., 2004. Retinoic acid regulates cell cycle progression and cell differentiation in human monocytic THP-1 cells. Exp Cell Res 297, 68–81. https://doi.org/10.1016/j.yexcr.2004.02.017

Chen, Y., Zhang, J., Ge, X., Du, J., Deb, D.K., Li, Y.C., 2013. Vitamin D receptor inhibits nuclear factor κb activation by interacting with IκB kinase β protein. Journal of Biological Chemistry 288, 19450–19458. https://doi.org/10.1074/jbc.M113.467670

Chiang, C., Beljanski, V., Yin, K., Olagnier, D., Ben Yebdri, F., Steel, C., Goulet, M.-L., DeFilippis, V.R., Streblow, D.N., Haddad, E.K., Trautmann, L., Ross, T., Lin, R., Hiscott, J., 2015. Sequence-Specific Modifications Enhance the Broad-Spectrum Antiviral Response Activated by RIG-I Agonists. J Virol 89, 8011–8025. https://doi.org/10.1128/jvi.00845-15

Choi, K.M., Kashyap, P.C., Dutta, N., Stoltz, G.J., Ordog, T., Shea Donohue, T., Bauer, A.J., Linden, D.R., Szurszewski, J.H., Gibbons, S.J., Farrugia, G., 2010. CD206-Positive M2 Macrophages That Express Heme Oxygenase-1 Protect Against Diabetic Gastroparesis in Mice. Gastroenterology 138. https://doi.org/10.1053/j.gastro.2010.02.014

Christakos, S., Dhawan, P., Verstuyf, A., Verlinden, L., Carmeliet, G., 2016. Vitamin D: Metabolism, Molecular Mechanism of Action, and Pleiotropic Effects. Physiol Rev 96, 365. https://doi.org/10.1152/PHYSREV.00014.2015

Colotta, F., Jansson, B., Bonelli, F., 2017. Modulation of inflammatory and immune responses by vitamin D. J Autoimmun. https://doi.org/10.1016/j.jaut.2017.07.007

Covarrubias, R., Ismahil, M.A., Rokosh, G., Hamid, T., Accornero, F., Singh, H., Gumina, R.J., Prabhu, S.D., Bansal, S.S., 2019. Optimized protocols for isolation, fixation, and flow cytometric characterization of leukocytes in ischemic hearts. INNOVATIVE METHODOLOGY Adaptive Immunity in Cardiovascular Disease Am J Physiol Heart Circ Physiol 317, 658–666. https://doi.org/10.1152/ajpheart.00137.2019.-Immune

Cutolo, M., 2008. Vitamin D or hormone D deficiency in autoimmune rheumatic diseases, including undifferentiated connective tissue disease. Arthritis Res Ther. https://doi.org/10.1186/ar2552

Daigneault, M., Preston, J.A., Marriott, H.M., Whyte, M.K.B., Dockrell, D.H., 2010. The identification of markers of macrophage differentiation in PMA-stimulated THP-1 cells and monocyte-derived macrophages. PLoS One 5. https://doi.org/10.1371/journal.pone.0008668

Davies, L.C., Jenkins, S.J., Allen, J.E., Taylor, P.R., 2013. Tissue-resident macrophages. Nat Immunol. https://doi.org/10.1038/ni.2705

de la Torre Lossa, P., Moreno Álvarez, M., González Guzmán, M. del C., López Martínez, R., Ríos Acosta, C., 2020. Vitamin D is not useful as a biomarker for disease activity

in rheumatoid arthritis. Reumatol Clin 16, 110–115. https://doi.org/10.1016/j.reuma.2018.02.016

Du, X., Qian, J., Wang, Y., Zhang, M., Chu, Y., Li, Y., 2019. Identification and immunological evaluation of novel TLR2 agonists through structure optimization of Pam3CSK4. Bioorg Med Chem 27, 2784–2800. https://doi.org/10.1016/j.bmc.2019.05.005

Duque, G.A., Descoteaux, A., 2014. Macrophage Cytokines: Involvement in Immunity and Infectious Diseases. Front Immunol 5. https://doi.org/10.3389/FIMMU.2014.00491

Epelman, S., Lavine, K.J., Randolph, G.J., 2014. Origin and Functions of Tissue Macrophages. Immunity. https://doi.org/10.1016/j.immuni.2014.06.013

Esteban, L., Vidal, M., Dusso, A., 2004. 1α-Hydroxylase transactivation by γ-interferon in murine macrophages requires enhanced C/EBPβ expression and activation, in: Journal of Steroid Biochemistry and Molecular Biology. pp. 131–137. https://doi.org/10.1016/j.jsbmb.2004.03.092

Ferrante, C.J., Pinhal-Enfield, G., Elson, G., Cronstein, B.N., Hasko, G., Outram, S., Leibovich, S.J., 2013. The adenosine-dependent angiogenic switch of macrophages to an M2-like phenotype is independent of interleukin-4 receptor alpha (IL-4Rα) signaling. Inflammation 36, 921–931. https://doi.org/10.1007/S10753-013-9621-3/FIGURES/6

Frega, G., Wu, Q., Le Naour, J., Vacchelli, E., Galluzzi, L., Kroemer, G., Kepp, O., 2020. Trial Watch: experimental TLR7/TLR8 agonists for oncological indications. Oncoimmunology. https://doi.org/10.1080/2162402X.2020.1796002

Funes, S.C., Rios, M., Escobar-Vera, J., Kalergis, A.M., 2018. Implications of macrophage polarization in autoimmunity. Immunology. https://doi.org/10.1111/imm.12910

Gabrilovich, D.I., Ostrand-Rosenberg, S., Bronte, V., 2012. Coordinated regulation of myeloid cells by tumours. Nat Rev Immunol. https://doi.org/10.1038/nri3175

Galli, S.J., Borregaard, N., Wynn, T.A., 2011. Phenotypic and functional plasticity of cells of innate immunity: Macrophages, mast cells and neutrophils. Nat Immunol. https://doi.org/10.1038/ni.2109

Genin, M., Clement, F., Fattaccioli, A., Raes, M., Michiels, C., 2015. M1 and M2 macrophages derived from THP-1 cells differentially modulate the response of cancer cells to etoposide. BMC Cancer 15. https://doi.org/10.1186/s12885-015-1546-9

Gordon, S., Martinez, F.O., 2010. Alternative Activation of Macrophages: Mechanism and Functions. Immunity 32, 593–604. https://doi.org/10.1016/J.IMMUNI.2010.05.007

Goulet, M.L., Olagnier, D., Xu, Z., Paz, S., Belgnaoui, S.M., Lafferty, E.I., Janelle, V., Arguello, M., Paquet, M., Ghneim, K., Richards, S., Smith, A., Wilkinson, P.,

Cameron, M., Kalinke, U., Qureshi, S., Lamarre, A., Haddad, E.K., Sekaly, R.P., Peri, S., Balachandran, S., Lin, R., Hiscott, J., 2013a. Systems Analysis of a RIG-I Agonist Inducing Broad Spectrum Inhibition of Virus Infectivity. PLoS Pathog 9. https://doi.org/10.1371/journal.ppat.1003298

Goulet, M.L., Olagnier, D., Xu, Z., Paz, S., Belgnaoui, S.M., Lafferty, E.I., Janelle, V., Arguello, M., Paquet, M., Ghneim, K., Richards, S., Smith, A., Wilkinson, P., Cameron, M., Kalinke, U., Qureshi, S., Lamarre, A., Haddad, E.K., Sekaly, R.P., Peri, S., Balachandran, S., Lin, R., Hiscott, J., 2013b. Systems Analysis of a RIG-I Agonist Inducing Broad Spectrum Inhibition of Virus Infectivity. PLoS Pathog 9. https://doi.org/10.1371/journal.ppat.1003298

Gui, B., Chen, Q., Hu, C., Zhu, C., He, G., 2017. Effects of calcitriol (1, 25-dihydroxy-vitamin D3) on the inflammatory response induced by H9N2 influenza virus infection in human lung A549 epithelial cells and in mice. Virol J 14, 1–11. https://doi.org/10.1186/s12985-017-0683-y

He, L., Jhong, J.H., Chen, Q., Huang, K.Y., Strittmatter, K., Kreuzer, J., DeRan, M., Wu, X., Lee, T.Y., Slavov, N., Haas, W., Marneros, A.G., 2021. Global characterization of macrophage polarization mechanisms and identification of M2-type polarization inhibitors. Cell Rep 37. https://doi.org/10.1016/j.celrep.2021.109955

Heaney, R.P., Horst, R.L., Cullen, D.M., Armas, L.A.G., 2009. Vitamin D3 Distribution and status in the body. J Am Coll Nutr 28, 252–256. https://doi.org/10.1080/07315724.2009.10719779

Hirayama, D., Iida, T., Nakase, H., 2018. The Phagocytic Function of Macrophage-Enforcing Innate Immunity and Tissue Homeostasis. Int J Mol Sci 19. https://doi.org/10.3390/IJMS19010092

Humeniuk-Polaczek, R., Marcinkowska, E., 2004. Impaired nuclear localization of vitamin D receptor in leukemia cells resistant to calcitriol-induced differentiation. Journal of Steroid Biochemistry and Molecular Biology 88, 361–366. https://doi.org/10.1016/j.jsbmb.2004.01.002

Imbeaud, S., Graudens, E., Boulanger, V., Barlet, X., Zaborski, P., Eveno, E., Mueller, O., Schroeder, A., Auffray, C., 2005. Towards standardization of RNA quality assessment using user-independent classifiers of microcapillary electrophoresis traces. Nucleic Acids Res 33, 1–12. https://doi.org/10.1093/nar/gni054

Jadhav, N.J., Gokhale, S., Seervi, M., Patil, P.S., Alagarasu, K., 2018. Immunomodulatory effect of 1, 25 dihydroxy vitamin D3 on the expression of RNA sensing pattern recognition receptor genes and cytokine response in dengue virus infected U937-DC-SIGN cells and THP-1 macrophages. Int Immunopharmacol 62, 237–243. https://doi.org/10.1016/j.intimp.2018.07.019

Jaguin, M., Houlbert, N., Fardel, O., Lecureur, V., 2013. Polarization profiles of human M-CSF-generated macrophages and comparison of M1-markers in classically activated macrophages from GM-CSF and M-CSF origin. Cell Immunol 281, 51–61. https://doi.org/10.1016/j.cellimm.2013.01.010

Jensen, J.B., Møller, A.B., Just, J., Mose, M., de Paoli, F. V., Billeskov, T.B., Fred, R.G., Pers, T.H., Pedersen, S.B., Petersen, K.K., Bjerre, M., Farup, J., Jessen, N., 2021. Isolation and characterization of muscle stem cells, fibro-adipogenic progenitors, and macrophages from human skeletal muscle biopsies. Am J Physiol Cell Physiol 321, C257–C268. https://doi.org/10.1152/ajpcell.00127.2021

Kamen, D.L., Tangpricha, V., 2010. Vitamin D and molecular actions on the immune system: Modulation of innate and autoimmunity. J Mol Med. https://doi.org/10.1007/s00109-010-0590-9

Krutzik, S.R., Hewison, M., Liu, P.T., Robles, J.A., Stenger, S., Adams, J.S., Modlin, R.L., 2008. IL-15 Links TLR2/1-Induced Macrophage Differentiation to the Vitamin D-Dependent Antimicrobial Pathway.

Kumar, H., Kawai, T., Akira, S., 2011. Pathogen recognition by the innate immune system. Int Rev Immunol 30, 16–34. https://doi.org/10.3109/08830185.2010.529976

L Bishop, E., Ismailova, A., Dimeloe, S., Hewison, M., White, J.H., 2021. Vitamin D and Immune Regulation: Antibacterial, Antiviral, Anti-Inflammatory, in: JBMR Plus. Blackwell Publishing Ltd. https://doi.org/10.1002/jbm4.10405

Lampiasi, N., Russo, R., Zito, F., 2016. The Alternative Faces of Macrophage Generate Osteoclasts. Biomed Res Int. https://doi.org/10.1155/2016/9089610

Lang, P.O., Samaras, N., Samaras, D., Aspinall, R., 2013. How important is vitamin D in preventing infections? Osteoporos Int 24, 1537–1553. https://doi.org/10.1007/S00198-012-2204-6

Lee, H.S., Stachelek, S.J., Tomczyk, N., Finley, M.J., Composto, R.J., Eckmann, D.M., 2013. Correlating macrophage morphology and cytokine production resulting from biomaterial contact. J Biomed Mater Res A 101 A, 203–212. https://doi.org/10.1002/jbm.a.34309

Lendeckel, U., Venz, S., Wolke, C., 2022. Macrophages: shapes and functions. ChemTexts 8, 12. https://doi.org/10.1007/S40828-022-00163-4

Lin, C.J., Martin, J.M., Cole, K.S., Zimmerman, R.K., Susick, M., Moehling, K.K., Levine, M.Z., Spencer, S., Flannery, B., Nowalk, M.P., 2017. Are children's vitamin D levels and BMI associated with antibody titers produced in response to 2014–2015 influenza vaccine? Hum Vaccin Immunother 13, 1661–1665. https://doi.org/10.1080/21645515.2017.1299837

Liu, G., Zhou, Y., 2019. Cytoplasm and Beyond: Dynamic Innate Immune Sensing of Influenza A Virus by RIG-I. J Virol 93. https://doi.org/10.1128/JVI.02299-18

Liu, G.Q., Lu, Y., Thulasi Raman, S.N., Xu, F., Wu, Q., Li, Z., Brownlie, R., Liu, Q., Zhou, Y., 2018. Nuclear-resident RIG-I senses viral replication inducing antiviral immunity. Nature Communications 2018 9:1 9, 1–14. https://doi.org/10.1038/s41467-018-05745-w

Liu, S., Yang, W., Li, Y., Sun, C., 2023. Fetal bovine serum, an important factor affecting the reproducibility of cell experiments. Sci Rep 13. https://doi.org/10.1038/s41598-023-29060-7

Liu, S.X., Gustafson, H.H., Jackson, D.L., Pun, S.H., Trapnell, C., 2020. Trajectory analysis quantifies transcriptional plasticity during macrophage polarization. Sci Rep 10. https://doi.org/10.1038/s41598-020-68766-w

Liu, T., Huang, T., Li, J., Li, A., Li, C., Huang, X., Li, D., Wang, S., Liang, M., 2023. Optimization of differentiation and transcriptomic profile of THP-1 cells into macrophage by PMA. PLoS One 18. https://doi.org/10.1371/journal.pone.0286056

Liu, W.S., Heckman, C.A., 1998. The Sevenfold Way of PKC Regulation, Cell. Signal.

Locati, M., Curtale, G., Mantovani, A., 2025. Diversity, Mechanisms, and Significance of Macrophage Plasticity. https://doi.org/10.1146/annurev-pathmechdis

Loeb, M., Dang, A.D., Thiem, V.D., Thanabalan, V., Wang, B., Nguyen, N.B., Tran, H.T.M., Luong, T.M., Singh, P., Smieja, M., Maguire, J., Pullenayegum, E., 2019. Effect of Vitamin D supplementation to reduce respiratory infections in children and adolescents in Vietnam: A randomized controlled trial. Influenza Other Respir Viruses 13, 176–183. https://doi.org/10.1111/irv.12615

Lund, M.E., To, J., O'Brien, B.A., Donnelly, S., 2016. The choice of phorbol 12-myristate 13-acetate differentiation protocol influences the response of THP-1 macrophages to a pro-inflammatory stimulus. J Immunol Methods 430, 64–70. https://doi.org/10.1016/j.jim.2016.01.012

Maeß, M.B., Wittig, B., Cignarella, A., Lorkowski, S., 2014. Reduced PMA enhances the responsiveness of transfected THP-1 macrophages to polarizing stimuli. J Immunol Methods 402, 76–81. https://doi.org/10.1016/j.jim.2013.11.006

Makaremi, S., Luu, H., Boyle, J.P., Zhu, Y., Cerson, C., Bowdish, D.M.E., Moran-Mirabal, J.M., 2019. The Topography of Silica Films Modulates Primary Macrophage Morphology and Function. Adv Mater Interfaces 6. https://doi.org/10.1002/admi.201900677

Mantovani, A., Sozzani, S., Locati, M., Allavena, P., Sica, A., 2002. Macrophage polarization: tumor-associated macrophages as a paradigm for polarized M2 mononuclear phagocytes, TRENDS in Immunology.

Martinez, F.O., Gordon, S., 2014. The M1 and M2 paradigm of macrophage activation: Time for reassessment. F1000Prime Rep 6. https://doi.org/10.12703/P6-13

McCartan, S., Powell, L.A., Green, B.D., McEneny, J., McGinty, A., 2015. The anti-atherogenic effects of eicosapentaenoic and docosahexaenoic acid are dependent on the stage of THP-1 macrophage differentiation. J Funct Foods 19, 958–969. https://doi.org/10.1016/j.jff.2014.12.023

Melbourne, J.K., Pang, Y., Park, M.R., Sudhalkar, N., Rosen, C., Sharma, R.P., 2020. Treatment with the antipsychotic risperidone is associated with increased M1-like JAK-STAT1 signature gene expression in PBMCs from participants with psychosis

and THP-1 monocytes and macrophages. Int Immunopharmacol 79. https://doi.org/10.1016/j.intimp.2019.106093

Menzies, F.M., Henriquez, F.L., Alexander, J., Roberts, C.W., 2011. Selective inhibition and augmentation of alternative macrophage activation by progesterone. Immunology 134, 281–291. https://doi.org/10.1111/j.1365-2567.2011.03488.x

Miller, R.L., Meng, T.C., Tomai, M.A., 2008. The antiviral activity of toll-like receptor 7 and 7/8 agonists. Drug News Perspect. https://doi.org/10.1358/dnp.2008.21.2.1188193

Mol, B.A., Wasinda, J.J., Xu, Y.F., Gentle, N.L., Meyer, V., 2024. 1,25-dihydroxyvitamin D3 augments low-dose PMA-based monocyte-to-macrophage differentiation in THP-1 cells. J Immunol Methods 532, 113716. https://doi.org/10.1016/j.jim.2024.113716

Moradian, H., Roch, T., Lendlein, A., Gossen, M., 2020. mRNA Transfection-Induced Activation of Primary Human Monocytes and Macrophages: Dependence on Carrier System and Nucleotide Modification. Sci Rep 10. https://doi.org/10.1038/s41598-020-60506-4

Morón-Calvente, V., Romero-Pinedo, S., Toribio-Castelló, S., Plaza-Díaz, J., Abadía-Molina, A.C., Rojas-Barros, D.I., Beug, S.T., LaCasse, E.C., MacKenzie, A., Korneluk, R., Abadía-Molina, F., 2018. Inhibitor of apoptosis proteins, NAIP, cIAP1 and cIAP2 expression during macrophage differentiation and M1/M2 polarization. PLoS One 13. https://doi.org/10.1371/journal.pone.0193643

Murray, P.J., 2017. Macrophage Polarization. Annu Rev Physiol 79, 541–566. https://doi.org/10.1146/ANNUREV-PHYSIOL-022516-034339/CITE/REFWORKS

Mytych, J., Romerowicz-Misielak, M., Koziorowski, M., 2017. Long-term culture with lipopolysaccharide induces dose-dependent cytostatic and cytotoxic effects in THP-1 monocytes. Toxicology in Vitro 42, 1–9. https://doi.org/10.1016/j.tiv.2017.03.009

Neuhaus, B., Tosun, B., Rotan, O., Frede, A., Westendorf, A.M., Epple, M., 2016. Nanoparticles as transfection agents: A comprehensive study with ten different cell lines. RSC Adv 6, 18102–18112. https://doi.org/10.1039/c5ra25333k

Nygaard, R.H., Nielsen, M.C., Antonsen, K.W., Højskov, C.S., Sørensen, B.S., Møller, H.J., 2022. Metabolism of 25-Hydroxy-Vitamin D in Human Macrophages Is Highly Dependent on Macrophage Polarization. Int J Mol Sci 23. https://doi.org/10.3390/ijms231810943

Oghogho Omage, S., Wallert, M., Lorkowski, S., 2024. Cell culture of THP-1 monocytes and differentiation into macrophages with PMA v1. https://doi.org/10.17504/protocols.io.5jyl8255dl2w/v1

Orlikowsky, T., Dannecker, G.E., Wang, Z.-Q., Horowitz, H., Niethammer, D., Hoffmann, M.K., 1999. Activation or Destruction of T Cells via Macrophages, Pathobiology.

O'Shea, J., Paul, W.E., 2010. Mechanisms underlying lineage commitment and plasticity of helper CD4 + T cells. Science (1979) 327, 1098–1102. https://doi.org/10.1126/SCIENCE.1178334/ASSET/6D2E92E2-30FB-4D92-8D44-C1A0FEFF75E7/ASSETS/GRAPHIC/327_1098_F2.JPEG

Oturai, D.B., Søndergaard, H.B., Börnsen, L., Sellebjerg, F., Romme Christensen, J., 2016. Identification of Suitable Reference Genes for Peripheral Blood Mononuclear Cell Subset Studies in Multiple Sclerosis. Scand J Immunol 83, 72–80. https://doi.org/10.1111/sji.12391

Park, E.K., Jung, H.S., Yang, H.I., Yoo, M.C., Kim, C., Kim, K.S., 2007. Optimized THP-1 differentiation is required for the detection of responses to weak stimuli. Inflammation Research 56, 45–50. https://doi.org/10.1007/s00011-007-6115-5

Parker, D., 2018. CD80/CD86 signaling contributes to the proinflammatory response of Staphylococcus aureus in the airway. Cytokine 107, 130–136. https://doi.org/10.1016/j.cyto.2018.01.016

Peng, Y., Zhou, M., Yang, H., Qu, R., Qiu, Y., Hao, J., Bi, H., Guo, D., 2023. Regulatory Mechanism of M1/M2 Macrophage Polarization in the Development of Autoimmune Diseases. Mediators Inflamm. https://doi.org/10.1155/2023/8821610

Pinto, S.M., Kim, H., Subbannayya, Y., Giambelluca, M., Bösl, K., Kandasamy, R.K., 2020. Dose-dependent phorbol 12-myristate-13-acetate-mediated monocyte-to-macrophage differentiation induces unique proteomic signatures in THP-1 cells. https://doi.org/10.1101/2020.02.27.968016

Pinto, S.M., Kim, H., Subbannayya, Y., Giambelluca, M.S., Bösl, K., Ryan, L., Sharma, A., Kandasamy, R.K., 2021. Comparative Proteomic Analysis Reveals Varying Impact on Immune Responses in Phorbol 12-Myristate-13-Acetate-Mediated THP-1 Monocyte-to-Macrophage Differentiation. Front Immunol 12. https://doi.org/10.3389/fimmu.2021.679458

Porta, C., Riboldi, E., Ippolito, A., Sica, A., 2015. Molecular and epigenetic basis of macrophage polarized activation. Semin Immunol 27, 237–248. https://doi.org/10.1016/J.SMIM.2015.10.003

Qin, Z., 2012. The use of THP-1 cells as a model for mimicking the function and regulation of monocytes and macrophages in the vasculature. Atherosclerosis. https://doi.org/10.1016/j.atherosclerosis.2011.09.003

Rajaiah, R., Perkins, D.J., Polumuri, S.K., Zhao, A., Keegan, A.D., Vogel, S.N., 2013. Dissociation of Endotoxin Tolerance and Differentiation of Alternatively Activated Macrophages. The Journal of Immunology 190, 4763–4772. https://doi.org/10.4049/jimmunol.1202407

Rehwinkel, J., Gack, M.U., 2020. RIG-I-like receptors: their regulation and roles in RNA sensing. Nature Reviews Immunology 2020 20:9 20, 537–551. https://doi.org/10.1038/s41577-020-0288-3

Roche, P.A., Furuta, K., 2015. The ins and outs of MHC class II-mediated antigen processing and presentation. Nat Rev Immunol. https://doi.org/10.1038/nri3818

Rojas, J.M., Sanz-Ortega, L., Mulens-Arias, V., Gutiérrez, L., Pérez-Yagüe, S., Barber, D.F., 2016. Superparamagnetic iron oxide nanoparticle uptake alters M2 macrophage phenotype, iron metabolism, migration and invasion. Nanomedicine 12, 1127–1138. https://doi.org/10.1016/j.nano.2015.11.020

Routley, C.E., Ashcroft, G.S., 2009. Effect of estrogen and progesterone on macrophage activation during wound healing. Wound Repair and Regeneration 17, 42–50. https://doi.org/10.1111/j.1524-475X.2008.00440.x

Rynikova, M., Adamkova, P., Hradicka, P., Stofilova, J., Harvanova, D., Matejova, J., Demeckova, V., 2023. Transcriptomic Analysis of Macrophage Polarization Protocols: Vitamin D3 or IL-4 and IL-13 Do Not Polarize THP-1 Monocytes into Reliable M2 Macrophages. Biomedicines 11. https://doi.org/10.3390/biomedicines11020608

Ryu, A.H., Eckalbar, W.L., Kreimer, A., Yosef, N., Ahituv, N., 2017. Use antibiotics in cell culture with caution: Genome-wide identification of antibiotic-induced changes in gene expression and regulation. Sci Rep 7. https://doi.org/10.1038/s41598-017-07757-w

Sadtler, K., Destefano, S., Fertil, D., Josyula, A., n.d. "The role of macrophage scavenger receptors in engineered biomaterial scaffold remodeling" mondreakest t faust.

Sanlier, N., Guney-Coskun, M., 2022. Vitamin D, the immune system, and its relationship with diseases. Egyptian Pediatric Association Gazette 2022 70:1 70, 1–12. https://doi.org/10.1186/S43054-022-00135-W

Santa, K., 2023. Macrophages: Phagocytosis, Antigen Presentation, and Activation of Immunity. https://doi.org/10.5772/intechopen.110832

Sarntivijai, S., Lin, Y., Xiang, Z., Meehan, T.F., Diehl, A.D., Vempati, U.D., Schürer, S.C., Pang, C., Malone, J., Parkinson, H., Liu, Y., Takatsuki, T., Saijo, K., Masuya, H., Nakamura, Y., Brush, M.H., Haendel, M.A., Zheng, J., Stoeckert, C.J., Peters, B., Mungall, C.J., Carey, T.E., States, D.J., Athey, B.D., He, Y., 2014. CLO: The cell line ontology. J Biomed Semantics 5. https://doi.org/10.1186/2041-1480-5-37

Schwende, H., Fitzke, E., Ambs, P., Dieter, P., 1996. Differences in the state of differentiation of THP-1 cells induced by phorbol ester and 1,25-dihydroxyvitamin D3. J Leukoc Biol 59, 555–561. https://doi.org/10.1002/jlb.59.4.555

Scott, T.E., Lewis, C. V., Zhu, M., Wang, C., Samuel, C.S., Drummond, G.R., Kemp-Harper, B.K., 2023. IL-4 and IL-13 induce equivalent expression of traditional M2 markers and modulation of reactive oxygen species in human macrophages. Sci Rep 13. https://doi.org/10.1038/s41598-023-46237-2

Shapouri-Moghaddam, A., Mohammadian, S., Vazini, H., Taghadosi, M., Esmaeili, S.A., Mardani, F., Seifi, B., Mohammadi, A., Afshari, J.T., Sahebkar, A., 2018. Macrophage plasticity, polarization, and function in health and disease. J Cell Physiol. https://doi.org/10.1002/jcp.26429

Shiratori, H., Feinweber, C., Luckhardt, S., Linke, B., Resch, E., Geisslinger, G., Weigert, A., Parnham, M.J., 2017. THP-1 and human peripheral blood mononuclear cell-

derived macrophages differ in their capacity to polarize in vitro. Mol Immunol 88, 58–68. https://doi.org/10.1016/j.molimm.2017.05.027

Siddiqui, M., Manansala, J.S., Abdulrahman, H.A., Nasrallah, G.K., Smatti, M.K., Younes, N., Althani, A.A., Yassine, H.M., 2020. Immune Modulatory Effects of Vitamin D on Viral Infections. Nutrients 12, 1–16. https://doi.org/10.3390/NU12092879

Sierra-Filardi, E., Nieto, C., Domínguez-Soto, Á., Barroso, R., Sánchez-Mateos, P., Puig-Kroger, A., López-Bravo, M., Joven, J., Ardavín, C., Rodríguez-Fernández, J.L., Sánchez-Torres, C., Mellado, M., Corbí, Á.L., 2014. CCL2 Shapes Macrophage Polarization by GM-CSF and M-CSF: Identification of CCL2/CCR2-Dependent Gene Expression Profile. The Journal of Immunology 192, 3858–3867. https://doi.org/10.4049/jimmunol.1302821

Smith, T.D., Tse, M.J., Read, E.L., Liu, W.F., 2016. Regulation of macrophage polarization and plasticity by complex activation signals. Integrative Biology (United Kingdom) 8, 946–955. https://doi.org/10.1039/c6ib00105j

Snegarova, V., Naydenova, D., 2020. Vitamin D: a Review of its Effects on Epigenetics and Gene Regulation. Folia Medica 62(4): 662-667 62, 662–667. https://doi.org/10.3897/FOLMED.62.E50204

Spano, A., Barni, S., Sciola, L., 2013. PMA withdrawal in PMA-treated monocytic THP-1 cells and subsequent retinoic acid stimulation, modulate induction of apoptosis and appearance of dendritic cells. Cell Prolif 46, 328–347. https://doi.org/10.1111/cpr.12030

Spano, A., Monaco, G., Barni, S., Sciola, L., 2007. Expression of cell kinetics and death during monocyte-macrophage differentiation: Effects of Actinomycin D and Vinblastine treatments. Histochem Cell Biol 127, 79–94. https://doi.org/10.1007/s00418-006-0227-9

Starr, T., Bauler, T.J., Malik-Kale, P., Steele-Mortimer, O., 2018. The phorbol 12-myristate-13-acetate differentiation protocol is critical to the interaction of THP-1 macrophages with Salmonella Typhimurium. PLoS One 13. https://doi.org/10.1371/journal.pone.0193601

Strober, W., 2015. Trypan Blue Exclusion Test of Cell Viability. Curr Protoc Immunol 111, A3.B.1-A3.B.3. https://doi.org/10.1002/0471142735.ima03bs111

Suski, M., Wiśniewska, A., Kuś, K., Kiepura, A., Stachowicz, A., Stachyra, K., Czepiel, K., Madej, J., Olszanecki, R., 2020. Decrease of the pro-inflammatory M1-like response by inhibition of dipeptidyl peptidases 8/9 in THP-1 macrophages – quantitative proteomics of the proteome and secretome. Mol Immunol 127, 193–202. https://doi.org/10.1016/j.molimm.2020.09.005

Svetlana, Z. V, Zubova, S. V, Radzyukevich, Y. V, Grachev, S. V, Prokhorenko, Isabela R, Radžukevič, J. V, Gračev, S. V, Prokhorenko, Izabela R, 2018. EFFECT OF VARIOUS AGENTS ON THE DIRECTION OF THP□1 CELL DIFFERENTIATION UTICAJ RAZLIČITIH AGENASA NA SMER THP□1

ĆELIJSKE DIFERENCIJACIJE. 36 / Ser J Exp Clin Res 19, 263–269. https://doi.org/10.2478/SJECR□2018□0029

Tan, Y., Kagan, J.C., 2014. A cross-disciplinary perspective on the innate immune responses to bacterial lipopolysaccharide. Mol Cell. https://doi.org/10.1016/j.molcel.2014.03.012

Tarique, A.A., Logan, J., Thomas, E., Holt, P.G., Sly, P.D., Fantino, E., 2015. Phenotypic,functional,and plasticity features of classical and alternatively activated human macrophages. Am J Respir Cell Mol Biol 53, 676–688. https://doi.org/10.1165/rcmb.2015-0012OC

Teh, Y.C., Ding, J.L., Ng, L.G., Chong, S.Z., 2019. Capturing the fantastic voyage of monocytes through time and space. Front Immunol. https://doi.org/10.3389/fimmu.2019.00834

Thoresen, D.T., Galls, D., Götte, B., Wang, W., Pyle, A.M., 2023. A rapid RIG-I signaling relay mediates efficient antiviral response. Mol Cell 83, 90-104.e4. https://doi.org/10.1016/j.molcel.2022.11.018

Tian, G., Liang, X., Chen, D., Mao, X., Yu, J., Zheng, P., He, J., Huang, Z., Yu, B., 2016. Vitamin D3 supplementation alleviates rotavirus infection in pigs and IPEC-J2 cells via regulating the autophagy signaling pathway. Journal of Steroid Biochemistry and Molecular Biology 163, 157–163. https://doi.org/10.1016/j.jsbmb.2016.05.004

TMS (2019). Sciencell human primary hepatic macrophages cell. (Online). Available at https://tms-lab.com/product/sciencell-human-primary-hepatic-marophages-cell/ (Accessed: 14 May 2025)

Tsai, C.F., Chen, J.H., Yeh, W.L., 2019. Pulmonary fibroblasts-secreted CXCL10 polarizes alveolar macrophages under pro-inflammatory stimuli. Toxicol Appl Pharmacol 380. https://doi.org/10.1016/j.taap.2019.114698

Tsuchiya, S., Yamabe, M., Yamaguchi, Y., Kobayashi, Y., Konno, T., Tada, K., 1980. Establishment and characterization of a human acute monocytic leukemia cell line (THP-1). Int J Cancer 26, 171–176. https://doi.org/10.1002/ijc.2910260208

Tulk, S.E., Liao, K.C., Muruve, D.A., Li, Y., Beck, P.L., MacDonald, J.A., 2015. Vitamin D3 metabolites enhance the NLRP3-dependent secretion of IL-1β from human THP-1 monocytic cells. J Cell Biochem 116, 711–720. https://doi.org/10.1002/jcb.24985

Valdés López, J.F., Urcuqui-Inchima, S., 2018. Synergism between phorbol-12-myristate-13-acetate and vitamin D3 in the differentiation of U937 cells to monocytes and macrophages. Morphologie 102, 205–218. https://doi.org/10.1016/j.morpho.2018.06.001

Van den Bossche, J., O'Neill, L.A., Menon, D., 2017. Macrophage Immunometabolism: Where Are We (Going)? Trends Immunol. https://doi.org/10.1016/j.it.2017.03.001

Van Dyken, S.J., Locksley, R.M., 2013. Interleukin-4-and interleukin-13-mediated alternatively activated macrophages: Roles in homeostasis and disease. Annu Rev Immunol. https://doi.org/10.1146/annurev-immunol-032712-095906

Vandesompele, J., De Preter, K., Pattyn, ilip, Poppe, B., Van Roy, N., De Paepe, A., Speleman, rank, 2002. Accurate normalization of real-time quantitative RT-PCR data by geometric averaging of multiple internal control genes.

Vembadi, A., Menachery, A., Qasaimeh, M.A., 2019. Cell Cytometry: Review and Perspective on Biotechnological Advances. Front Bioeng Biotechnol. https://doi.org/10.3389/fbioe.2019.00147

Vogelpoel, L.T.C., Hansen, I.S., Rispens, T., Muller, F.J.M., Van Capel, T.M.M., Turina, M.C., Vos, J.B., Baeten, D.L.P., Kapsenberg, M.L., De Jong, E.C., Den Dunnen, J., 2014. Fc gamma receptor-TLR cross-talk elicits pro-inflammatory cytokine production by human M2 macrophages. Nat Commun 5. https://doi.org/10.1038/ncomms6444

Wang, L. xun, Zhang, S. xi, Wu, H. juan, Rong, X. lu, Guo, J., 2019. M2b macrophage polarization and its roles in diseases. J Leukoc Biol 106, 345–358. https://doi.org/10.1002/JLB.3RU1018-378RR

Wang, L., Zhang, Y., Zhang, N., Xia, J., Zhan, Q., Wang, C., 2019. Potential role of M2 macrophage polarization in ventilator-induced lung fibrosis. Int Immunopharmacol 75. https://doi.org/10.1016/j.intimp.2019.105795

Wang, N., Liang, H., Zen, K., 2014. Molecular mechanisms that influence the macrophage M1-M2 polarization balance. Front Immunol 5, 113523. https://doi.org/10.3389/FIMMU.2014.00614/BIBTEX

Weisser, S.B., McLarren, K.W., Kuroda, E., Sly, L.M., 2013. Generation and characterization of murine alternatively activated macrophages. Methods in Molecular Biology 946, 225–239. https://doi.org/10.1007/978-1-62703-128-8_14

White, J.H., 2012. Vitamin D metabolism and signaling in the immune system. Rev Endocr Metab Disord 13, 21–29. https://doi.org/10.1007/S11154-011-9195-Z

Wu, W., Zhang, W., Alexandar, J.S., Booth, J.L., Miller, C.A., Xu, C., Metcalf, J.P., 2023. RIG-I agonist SLR10 promotes macrophage M1 polarization during influenza virus infection. Front Immunol 14. https://doi.org/10.3389/fimmu.2023.1177624

Wynn, T.A., Vannella, K.M., 2016. Macrophages in Tissue Repair, Regeneration, and Fibrosis. Immunity. https://doi.org/10.1016/j.immuni.2016.02.015

Xu, Z.J., Gu, Y., Wang, C.Z., Jin, Y., Wen, X.M., Ma, J.C., Tang, L.J., Mao, Z.W., Qian, J., Lin, J., 2020. The M2 macrophage marker CD206: a novel prognostic indicator for acute myeloid leukemia. Oncoimmunology 9. https://doi.org/10.1080/2162402X.2019.1683347

Xuan, W., Qu, Q., Zheng, B., Xiong, S., Fan, G.-H., 2015. The chemotaxis of M1 and M2 macrophages is regulated by different chemokines. J Leukoc Biol 97, 61–69. https://doi.org/10.1189/jlb.1a0314-170r

Xue, J., Schmidt, S. V., Sander, J., Draffehn, A., Krebs, W., Quester, I., DeNardo, D., Gohel, T.D., Emde, M., Schmidleithner, L., Ganesan, H., Nino-Castro, A., Mallmann, M.R., Labzin, L., Theis, H., Kraut, M., Beyer, M., Latz, E., Freeman,

T.C., Ulas, T., Schultze, J.L., 2014. Transcriptome-Based Network Analysis Reveals a Spectrum Model of Human Macrophage Activation. Immunity 40, 274–288. https://doi.org/10.1016/j.immuni.2014.01.006

Yao, Y., Xu, X.H., Jin, L., 2019. Macrophage polarization in physiological and pathological pregnancy. Front Immunol. https://doi.org/10.3389/fimmu.2019.00792

Zhang, Y., Leung, D.Y.M., Richers, B.N., Liu, Y., Remigio, L.K., Riches, D.W., Goleva, E., 2012. Vitamin D Inhibits Monocyte/macrophage Pro-inflammatory Cytokine Production by Targeting Mitogen-Activated Protein Kinase Phosphatase 1. J Immunol 188, 2127. https://doi.org/10.4049/JIMMUNOL.1102412

Zhao, Z., Zhong, L., Li, P., He, K., Qiu, C., Zhao, L., Gong, J., 2020. Cholesterol impairs hepatocyte lysosomal function causing M1 polarization of macrophages via exosomal miR-122-5p. Exp Cell Res 387. https://doi.org/10.1016/j.yexcr.2019.111738

Zhou, Y., Yoshida, S., Nakao, S., Yoshimura, T., Kobayashi, Y., Nakama, T., Kubo, Y., Miyawaki, K., Yamaguchi, M., Ishikawa, K., Oshima, Y., Akashi, K., Ishibashi, T., 2015. M2 macrophages enhance pathological neovascularization in the mouse model of oxygen-induced retinopathy. Invest Ophthalmol Vis Sci 56, 4767–4777. https://doi.org/10.1167/iovs.14-16012

Zhu, J., Deluca, H.F., 2012. Vitamin D 25-hydroxylase - Four decades of searching, are we there yet? Arch Biochem Biophys. https://doi.org/10.1016/j.abb.2012.01.013

Zizzo, G., Hilliard, B.A., Monestier, M., Cohen, P.L., 2012. Efficient Clearance of Early Apoptotic Cells by Human Macrophages Requires M2c Polarization and MerTK Induction. The Journal of Immunology 189, 3508–3520. https://doi.org/10.4049/JIMMUNOL.1200662

APPENDICES

Appendix 1:

A

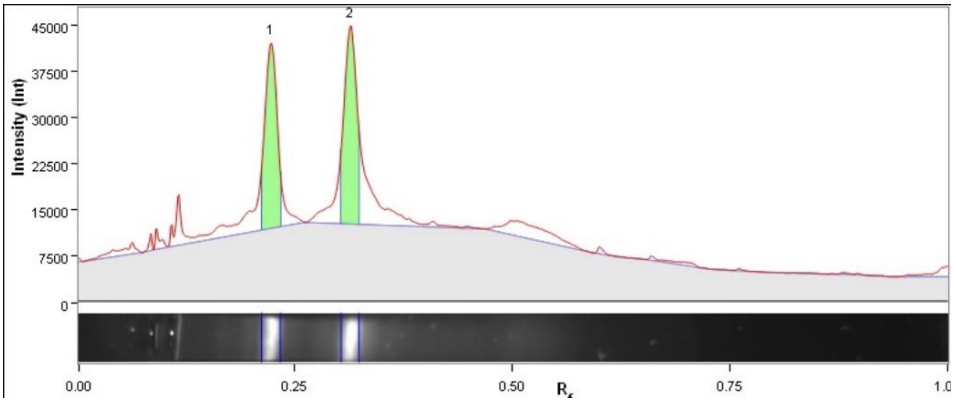

B

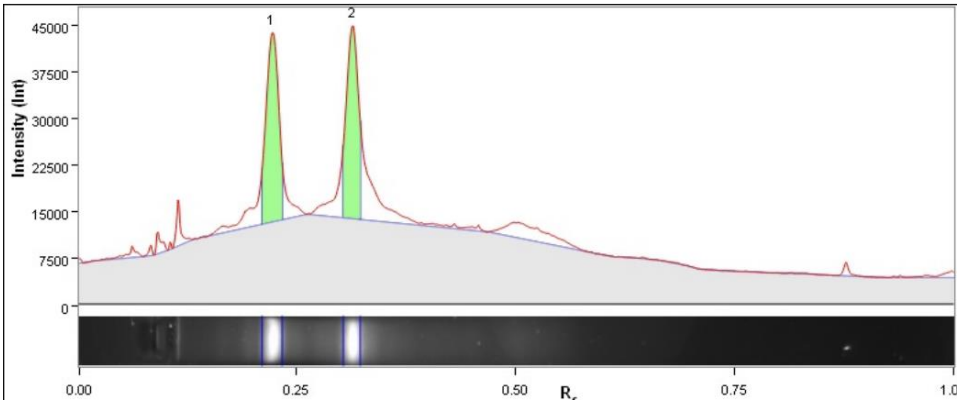

C

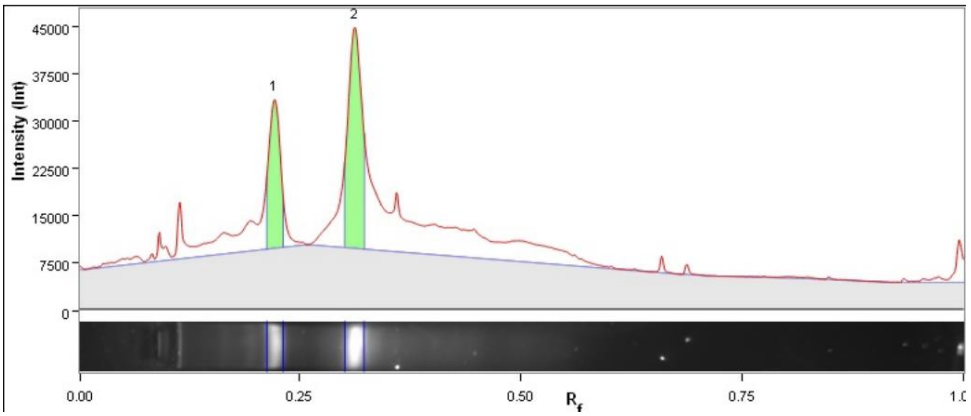

D

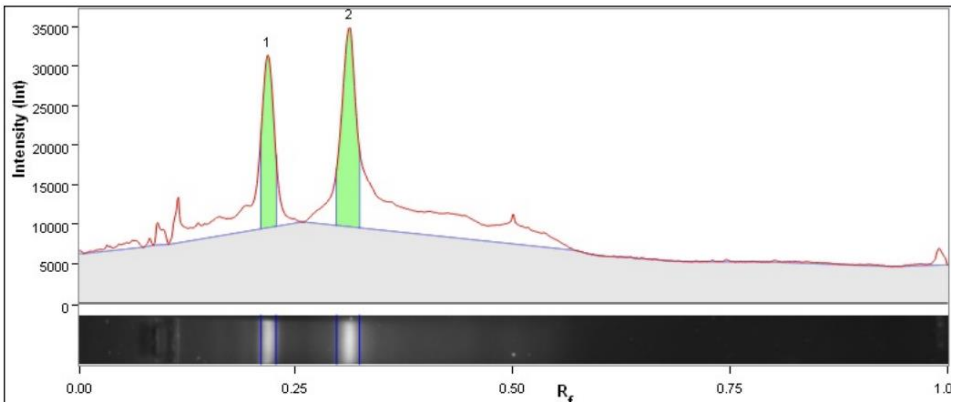

E

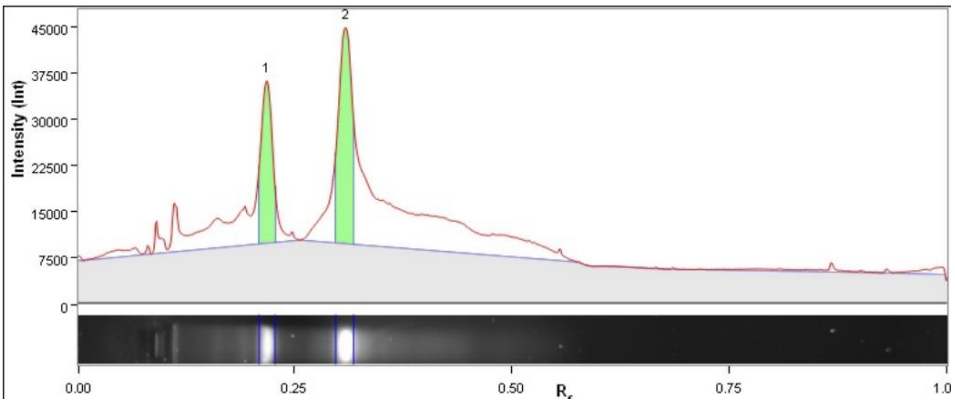

Figure A: 28S and 18S band intensity assessments. Graph images obtained from the Bio-Rad ChemiDoc XRS+ System with Image Lab Software showing the intensity (Int) against relative front (R_f). The images showed two peaks representing 28S (1) and 18S (2) for lanes representing the treatment conditions of macrophages, including treatment with A (control), B (5'ppp-dsRNA), C (5'ppp-dsRNA and 1,25D_3), D (1,25D_3), E (Lyovec).